EUROPEAN COMMISSION

Community research

GOBIERNO DE ESPAÑA | MINISTERIO DE ECONOMÍA Y COMPETITIVIDAD | Ciemat Centro de Investigaciones Energéticas, Medioambientales y Tecnológicas

PEBS Long-term Performance of Engineered Barrier Systems

Long-term Performance of Engineered Barrier Systems PEBS

Long-term THM tests reports:
Isothermal infiltration tests with materials from the HE-E

(DELIVERABLE-N°: D2.2-7.2)

Contract (grant agreement) number: FP7 249681

CIEMAT Technical Report CIEMAT/DMA/2G210/07/2013

Author(s):

M.V. Villar

Date of issue of this report: December 2nd 2013

Start date of project: 01/03/10 Duration : 48 Months

Project co-funded by the European Commission under the Seventh Euratom Framework Programme for Nuclear Research &Training Activities (2007-2011)		
Dissemination Level		
PU	Public	**PU**
RE	Restricted to a group specified by the partners of the [acronym] project	
CO	Confidential, only for partners of the [acronym] project	

EURATOM

Contents

Contents I

1 Introduction 1

2 Material 2

3 Methodology 6

3.1 Experimental setup 6

3.2 Post-mortem analysis 7

3.2.1 Pore size distribution 7

3.2.2 X-ray diffraction 8

4 Results 8

4.1 Tests with the sand/bentonite mixture 9

4.1.1 Test MGR15 9

4.1.2 Test MGR16 12

4.1.3 Test MGR19 16

4.2 Tests with bentonite pellets 18

4.2.1 Test MGR17 18

4.2.2 Test MGR18 21

5 Summary and conclusions 26

Acknowledgements 31

References 31

1 Introduction

A common design of a high-level radioactive waste (HLW) disposal system consists of the wastes encapsulated within steel canisters that are emplaced within horizontal tunnels, with the space between the canisters and the surrounding rock filled with a bentonite-based material. In the early post closure period the buffer is expected to experience the maximum temperature. In this phase the buffer is largely unsaturated and the thermal evolution of the EBS is likely to be controlled by the effective thermal conductivity of dry buffer.

In particular, the temperature evolution of the engineered barrier system and surrounding rock was simulated using reference data for the thermal properties of HLW, bentonite backfill and Opalinus Clay. The results showed that the surface temperatures would reach a maximum value of ~150°C within a few years after emplacement (Johnson *et al*. 2002). These anticipated temperatures at the canister surface, in the bentonite and at the bentonite-host rock interface were scaled down in time and space to meet the specifications of the HE-E experiment, which is being carried out in the framework of PEBS (Gaus *et al*. 2011). The HE-E experiment targets the period immediately after repository closure when the temperatures are maximal and the moisture content is low but increasing.

The HE-E experiment is a 1:2 scale heating experiment considering natural resaturation of the EBS and a maximum heater surface temperature of 140°C. Heater temperature is foreseen to increase almost linearly to its maximum value in a period of 1 year after which the temperature will be held constant for the years to follow. The experiment is located at the Mont Terri URL (Switzerland) in a 50-m long non-lined horizontal microtunnel of 1.3 m diameter excavated in 1999 in the shaly facies of the Opalinus Clay. The test section of the microtunnel was characterised in detail during the Ventilation Experiment (ENRESA 2005). The detailed design of the experiment is described in Teodori & Gaus (2011).

The experiment consists of two independently heated sections (Figure 1), where the heaters are placed in a steel liner supported by MX80 bentonite blocks (dry density 1.8 g/cm^3, water content 11%). The two sections are fully symmetric apart from the granular filling material: whereas section one is filled with pure MX80 bentonite pellets, section 2 is filled with a 65/35 granular sand/bentonite mixture with the characteristics described below:

- granular bentonite (B) and bentonite blocks are used in one section of the test, corresponding to the Swiss disposal concept. It is the same as the one used for the ESDRED project, mixture type E (sodium bentonite MX-80 from Wyoming). The material is described in detail in Plötze & Weber (2007). Once emplaced its water content was 5.9% and the dry average density was 1.46 kg/m^3.
- sand/bentonite (S/B) mixture (having a higher thermal conductivity) and bentonite blocks are used in the other section. The sand/bentonite mixture was provided by MPC (Limay, France). The components are 65 % of quartz sand with a grain spectrum of 0.5 – 1.8 mm and 35 % of sodium bentonite GELCLAY WH2 (granular material of the same composition as MX-80) of the same grain spectrum, which was obtained by crushing and sieving from the qualified raw material. Water content was 13 % for the bentonite and 0.05 % for the sand, giving a total water content of the mixture in the range of 4%. There is some uncertainty about the actual emplaced density of the mixture, and values as low as 1.26 g/cm^3 have been given. However, based on the tests performed to check the emplacement technique, a value of 1.5 g/cm^3 has been taken for the calculations and the laboratory tests.

A heater system, capable of representing the temperature curve of the anticipated heat production in the canisters (up to a maximum of 140°C), was switched on the 28th June 2011. During the experiment the temperature, humidity and the water saturation are monitored through a system of sensors on the heater surface within the liner, in the bentonite and in the surrounding host rock.

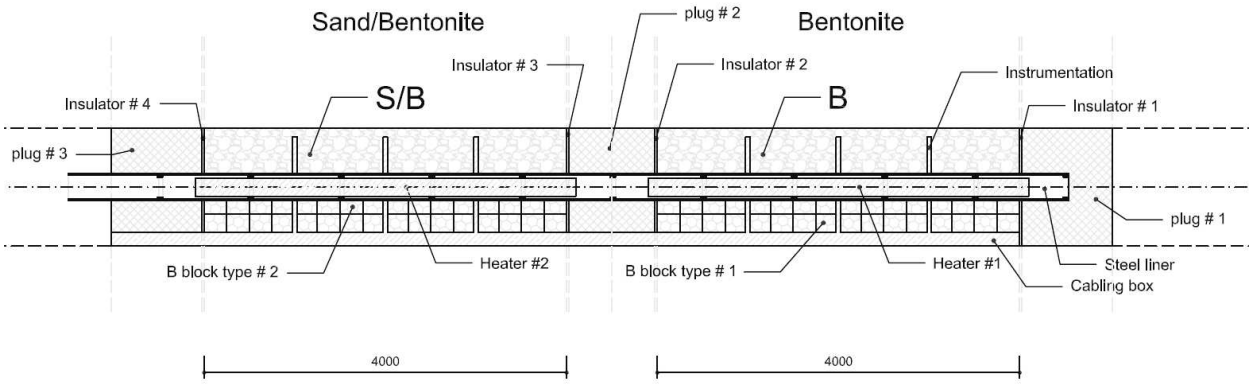


Figure 1: Layout of the *in situ* HE-E experiment

The performance of tests at different scales, in both the laboratory and the field, is very useful to observe the thermo-hydro-mechanical processes taking place in the engineered barriers and the geological medium. They also provide the information required for the verification and validation of mathematical models of the coupled processes and their numerical implementation. The laboratory tests in cells are particularly helpful to identify and quantify processes in a shorter period of time and with less uncertainty regarding the boundary conditions than the *in situ* tests. In the tests in cells the sealing material is subjected simultaneously to heating and hydration in opposite directions, in order to simulate the conditions of the clay barrier in the repository. With the aim of helping to understand the information provided by the HE-E *in situ* test, CIEMAT undertook, in the framework of the PEBS project, the performance of two tests in cells simulating the conditions of the sealing materials used in the two sections of the *in situ* test (Villar et al. 2012). To complement the knowledge gained with these TH tests, infiltration tests at room temperature were performed in a large scale oedometer. This would help telling apart the effects caused by the thermal gradient from those purely hydraulic. This report presents the results of the five isothermal tests performed with the materials used in the HE-E experiment.

2 Material

The materials used in the laboratory tests are the same as those used in the *in situ* test and were sent to CIEMAT directly from the Mont Terri test site. A plastic bucket with 25 kg of the sand/bentonite mixture (S/B) was received at CIEMAT on April 2011 and 20 kg of the bentonite pellets (B) were received on June 2011 (Figure 2). The as-received water content of the materials was 6.4% for the pellets and 3.6% for the sand/bentonite mixture. The granulometric curve of both materials obtained by dry sieving is shown in Figure 3. It was checked that the granulometric curve of the granular bentonite received at CIEMAT coincide with the granulometric curves of the material used for the ESDRED experiment (Figure 4).



Figure 2: Appearance of the materials received at CIEMAT: MX-80 pellets (left) and sand/bentonite mixture (right)

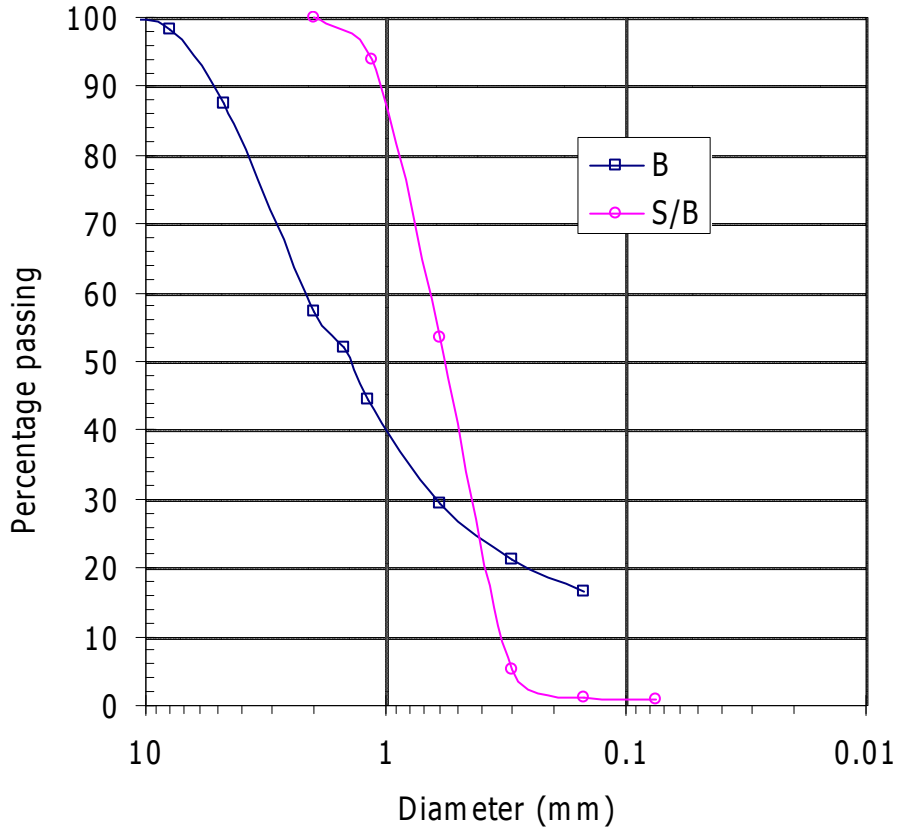


Figure 3: Granulometric curve obtained by dry sieving of the two materials used in the tests (B: bentonite pellets, S/B: sand/bentonite mixture)

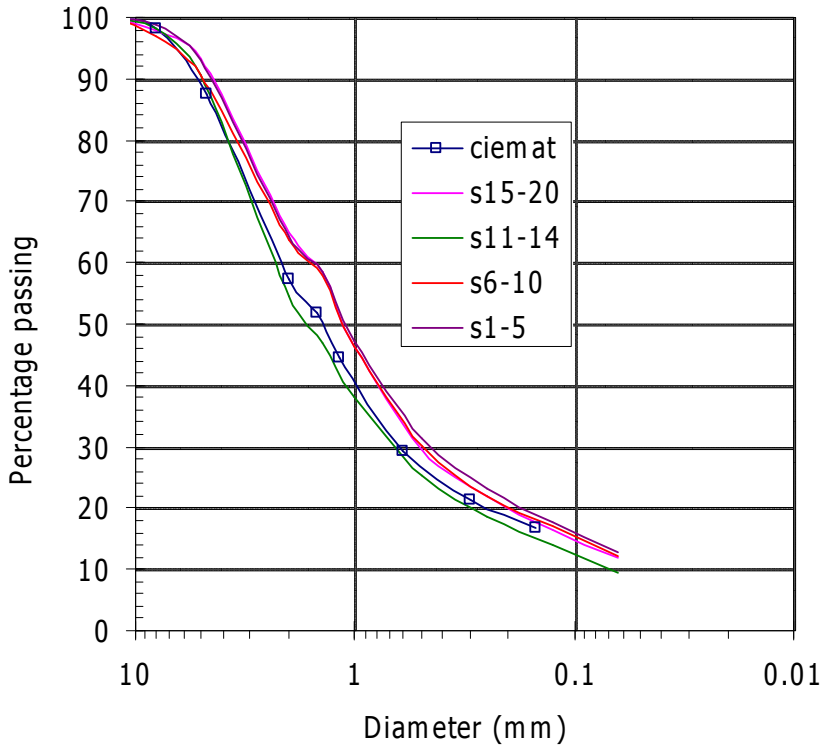


Figure 4: Comparison of the granulometric curve obtained at CIEMAT for the bentonite granulate and those obtained by NAGRA in material of the ESDRED test

The dry density of the solid grains determined with pycnometers using water as dispersing agent was 2.71 g/cm^3 for the mixture and 2.75 g/cm^3 for the granulate. The external specific surface area determined by the 9-point BET method was 5 m^2/g for the mixture and 33 m^2/g for the pellets. The superficial thermal conductivity of both materials in their as-received state was determined at room temperature using the transient hot wire method. Values of 0.33 and 0.12 W/m·K were obtained for the mixture and the granulate, respectively. The specific heat capacity of both materials ground and dried at 110°C was determined in a TG-DSC Setsys Evolution 16 equipment. The determinations were performed in the range of temperatures from 22 to 298°C. The values obtained for the mixture ranged between 0.74 J/g·K (at 22°C) and 0.90 J/g·K (at 115°C), and for the pellets between 0.64 J/g·K (at 22°C) and 0.97 J/g·K (at 115°C) (Fernández 2011).

The pore size distribution of the uncompacted materials was obtained by mercury intrusion porosimetry (MIP) and is shown in Figure 5. The difference between both is obvious, the S/B mixture having a predominant macroporosity with a pore mode about 204 µm whereas in the B pellets mesopores of pore mode about 0.014 µm predominate.

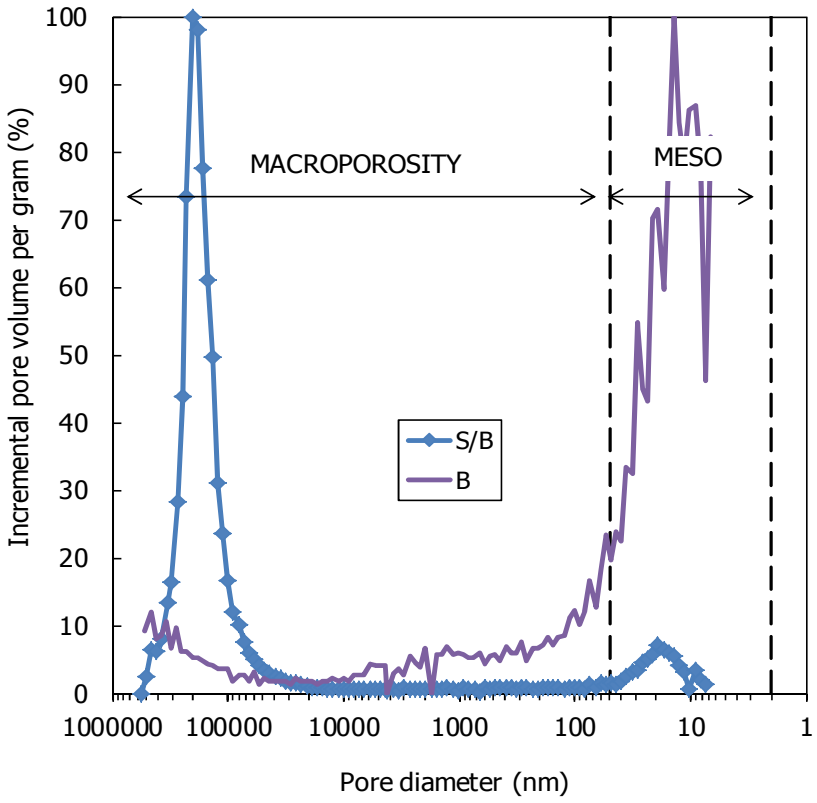


Figure 5: Pore size distribution obtained by MIP of the sand/bentonite mixture (S/B) and the bentonite pellets (B)

The swelling pressure of small samples (3.8 or 5.0 cm in diameter, 1.2 cm in height) of MX-80 bentonite powder compacted with its hygroscopic water content were determined at CIEMAT at room temperature using deionised water as saturation fluid. The swelling pressure (P_s, MPa) could be related to final dry density (ρ_d, g/cm^3) through the following equation:

$$\ln P_s = 5.44\ \rho_d - 6.94 \qquad [1]$$

Although these tests were performed in powder material with a grain size <1 mm, it was proved that the saturated hydro-mechanical properties of large pellets mixtures are similar to those of fine granulates (Imbert & Villar 2006).

The swelling pressure of the sand/bentonite mixture was determined in the same standard oedometers in samples initially compacted at a nominal dry density of 1.45 g/cm^3. Two tests were performed using deionised water to saturate the samples and two other using Pearson water. This solution is sodium rich and has a composition similar to the Opalinus Clay formation pore water. This water has a density of 1.020 g/cm^3 (Pearson 1998, Pearson *et al*. 1999). The chemical composition is indicated in Table I. An average swelling pressure of 1.5 MPa was obtained for the samples saturated with deionised water and of 0.7 MPa for the samples saturated with Pearson water.

Table I: Chemical composition of the water used in the tests (mg/L)

Cl^-	SO_4^{2-}	HCO_3^-	Mg^{2+}	Ca^{2+}	Na^+	K^+	Sr^+	pH
10635.90	1354.41	25.75	413.19	1034.06	5550.01	62.95	44.69	7.6

3 Methodology

3.1 EXPERIMENTAL SETUP

The large-scale oedometer was specially designed to work with pellets/powder mixtures and it consists of a cylindrical body with base and an upper piston that may move in the cylinder (Imbert & Villar 2006). The body has an inner diameter of 10.0 cm and the length of the sample inside may be 10 or 5 cm. The top and bottom of the sample are in contact with ceramic porous discs connected to outlets. The cell was placed in a rigid frame that guaranteed the constant volume of the sample by hindering the displacement of the piston. An external LVDT measured the potential axial displacements, whereas a load cell in the upper part of the frame measured the force developed by the specimen. This could be a 10-t or a 2-t cell, and it was changed depending on the expected swelling pressure.

The water intake, which took place thorough the bottom surface, was measured by an automatic volume change apparatus. The saturation system consisted of a water deposit placed 1.4 m above the base of the oedometer (Figure 7). It was connected to a volume change apparatus whose outlet was in turn connected to a deposit with a membrane inside separating the deionised water of the column from the Pearson water entering the oedometer. In this way the volume change apparatus was protected from corroding or precipitation of salts. In advanced stages of some tests the water column was replaced by a pressure system (oil/water pump or pressure/volume controller).

Once in the oedometer frame, the samples were saturated by the bottom face, while the top outlet remained initially open to atmosphere and the pressure exerted by the material, the sample deformation and the water intake were measured and automatically recorded. The tests were performed at laboratory temperature.

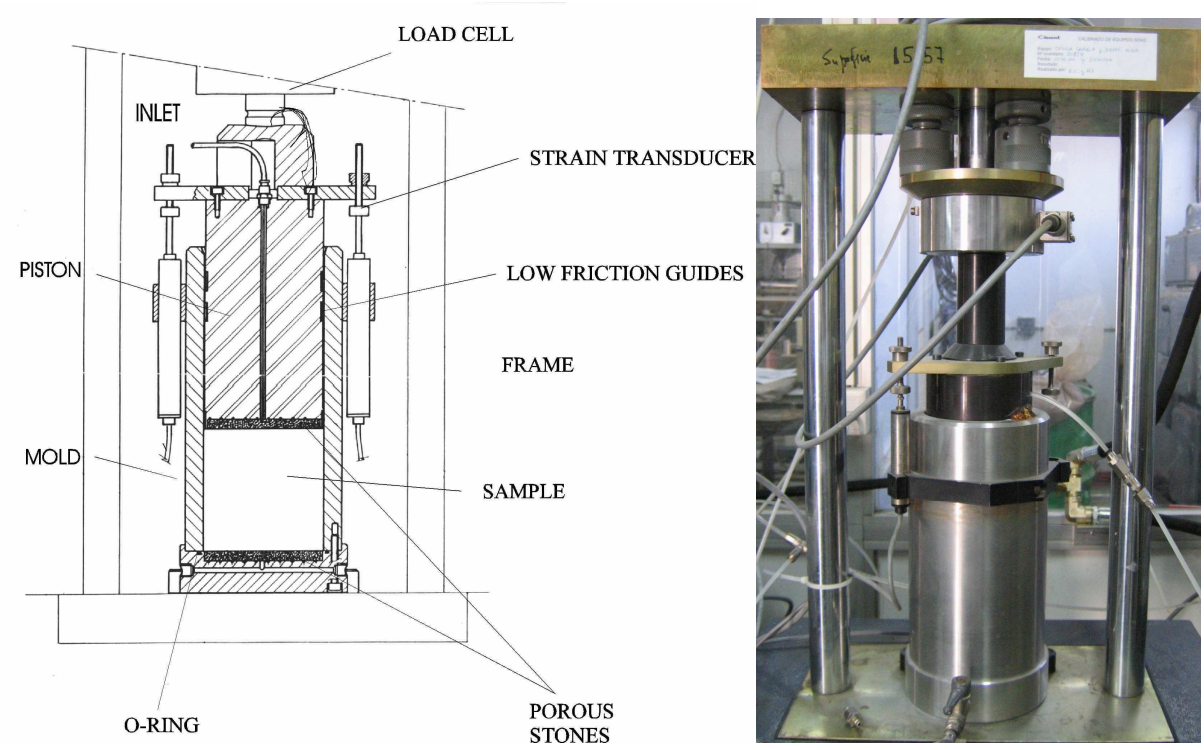


Figure 6: Schematic design and appearance of the large oedometric cell

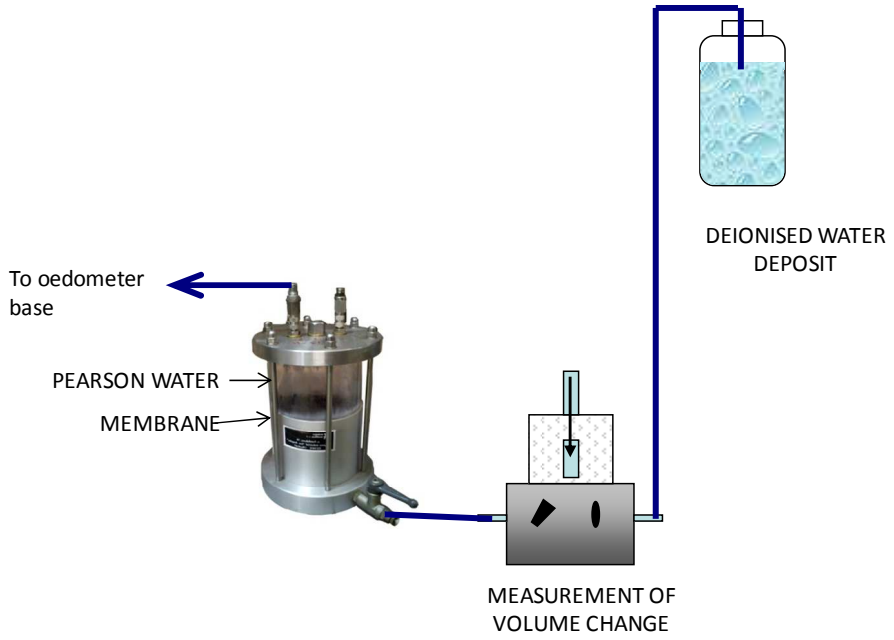


Figure 7: Setup for the saturation of the oedometer

3.2 POST-MORTEM ANALYSIS

After dismantling, the cylindrical samples were subsampled to determine the water content and dry density at different levels.

The gravimetric water content (*w*) is defined as the ratio between the weight of water and the weight of dry solid expressed as a percentage. The weight of water was determined as the difference between the weight of the sample and its weight after oven drying at 110°C for 48 h. Dry density (ρ_d) is defined as the ratio between the weight of the dry sample and the volume occupied by it prior to drying. The volume of the specimens was determined by immersing them in a recipient containing mercury and by weighing the mercury displaced, as established in UNE Standard 7045 "Determination of soil porosity".

Mercury intrusion porosimetry tests and measurement of the basal spacing of the smectite were done the subsamples of test MGR18 according to the procedures described below.

3.2.1 Pore size distribution

The pore size distribution was determined by mercury intrusion porosimetry (MIP) in subsamples from test MGR18. This technique allows the determination of pore size distribution by injecting mercury into the sample at different pressures while controlling the volume intruded. The pressure applied may be related to the minimum pore diameter intruded, taking into account the characteristics of the fluid. The ratio of the volume of mercury intruded (pore volume) to applied pressure (which conditions the minimum pore diameter) allows distribution curves to be obtained establishing the percentage of pores of a size included within a given range.

Samples of sizes lower than 3 cm^3 were cut and put in the ice condenser of a Telstar LioQuest equipment at -50°C for 3 h. Afterwards they were lyophilised for 19 h at a temperature of -50°C under a vacuum of 0.2 mbar, so that to eliminate the water in the pores by sublimation. Before the MIP tests the samples were heated to 35°C for 2 h. The porosimeter used was a Micromeritics AutoPore Series IV 9500, which applied a maximum injection pressure of 31900 psi, allowing the exploration of pore diameters between 0.007 and 500 µm. Prior to mercury

injection the sample was outgassed by applying a vacuum of 50 µmHg. Afterwards the mercury injection pressure was increased from 0.36 to 31900 psi in 110 steps. To determine the extrusion branch of the curve, the pressure was released in 57 steps down to a pressure of 4.44 psi. A contact angle of mercury of 139° both on advancing and of receding on the clay surface was considered.

The mercury does not intrude the microporosity (pores of a size of less than 0.002 µm, according to the classification of Sing *et al*. 1985), but only the macroporosity and part of the mesopores. The percentage of pores not intruded by mercury includes not only those whose sizes are below 0.007 µm or above 500 µm, but also those whose entrance pore size is below that value or those isolated, even if the pores themselves are larger. The percentage of pores not intruded can be computed by comparing the actual void ratio of the samples (computed from their dry density and solid specific gravity measured by pycnometers) and the apparent void ratio calculated from mercury intrusion. Then, assuming that the percentage of pores not intruded in a clay corresponds entirely to the micropore size, the percentage of micropores can be estimated. Alternatively, Delage & Lefebvre (1984) suggested that microporosity could be estimated from the trapped volumes after mercury extrusion.

3.2.2 X-ray diffraction

X-ray profiles were registered in the samples to determine the smectite basal spacing. For that, the X-ray profiles of a sufficiently flat surface of the samples were registered at room temperature without any previous treatment. An anticatode of Cu (CuK_α) radiation was used with a Philips model X'Pert-MPD diffractometer at 40 mA, 45 kV operating condition. X-ray diffraction (XRD) experimental profiles were obtained with a 0.1 mm entrance slit and a scanning rate of 0.02 °2θ/s. Data were collected from 0.2 to 30 °2θ. The position of the peaks was adjusted by using the quartz in the samples as an internal standard. A profile function was fitted to the observed intensities in order to obtain better peak parameters (peak position, net intensity and full width at half maximum (FWHM)) completely describing the measured scan. The pseudo-Voigt profile function, which is the weighted mean between a Lorentz and a Gaussian function, was used. It was also used to deconvolute overlapped peaks.

4 Results

Five tests were performed in the large oedometer cell described in section 3.1. In all of them the dimensions of the cylindrical specimens were 10 cm in diameter and 10 cm in nominal height and Pearson water (Table I) was used as saturating fluid. For the sand/bentonite mixture (S/B) the initial nominal dry density and water content were 1.45 g/cm^3 and 3.6%, and for the bentonite pellets (B) were 1.47 g/cm^3 and 6.3%, respectively. These values were checked at the end of the tests and the actual values are those indicated in Table II, in which other particular characteristics of each test are shown.

Table II: Characteristics of the tests performed

Reference	Material	Initial ρ_d (g/cm^3)	Initial *w* (%)	Initial S_r (%)	Load cell	Water *P* (kPa)	Duration (days)	*T* (°C)
MGR15	S/B	1.47	2.2	7	10-t	1.4 / 200	51	24.1±0.9
MGR16	S/B	1.46	2.9	9	2-t	1.4	41	23.8±0.9
MGR17	B	1.47	5.9	19	2-t / 10-t	1.4	118	22.0±2.0
MGR18	B	1.47	6.1	19	10-t	1.4 / 200 / 600	446	23.5±2.6
MGR19	S/B	1.45	3.7	11	2-t	1.4 / 200	144	23.8±1.1

4.1 TESTS WITH THE SAND/BENTONITE MIXTURE

4.1.1 Test MGR15

The sand/bentonite mixture was introduced inside the cell in spoonfuls and compacted inside the cell by applying a uniaxial pressure of 3 MPa. The load cell used in the setup was the 10-t one.

4.1.1.1 ONLINE MEASUREMENTS

The test started in June 2011 using a 1.4-m water column to saturate the sample. Initially the upper outlet was open to atmosphere, but after just 3 h of testing it had to be closed because water was going out through it. During the first days there were several leaks and the hydration inlet had to be closed. The leaks took place between the cell wall and the piston, and were manifested by water going up through this interface, which left salt precipitates upon evaporation (Figure 8). Consequently, the water intake measurement was overestimated, since it included not only the water taken by the sample but also the leak. Also, for an undetermined period of time before day 32 the hydration inlet remained closed. After 36 days the injection pressure was increased to 200 kPa. Figure 9 shows the evolution of water intake and axial pressure during the test. The thick vertical lines indicate the events commented above. It can be observed that most water intake took place in the first hours and that the sample barely developed pressure on saturation. The increase of water injection pressure to 200 kPa implied a sudden increase of water intake and pressure. Figure 10 shows how the evolution of axial pressure can be mainly related to the room temperature changes and to the increase in water injection pressure. Before the water pressure increase, the average axial pressure measured was 0.01 MPa, but there was not much accuracy in this measurement because the range of the load cell was too large for such low pressure values.

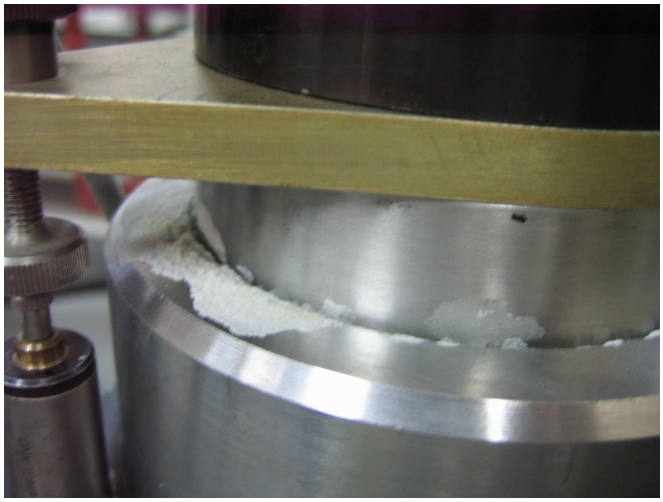


Figure 8: Salt precipitate in the upper part of the oedometer caused by the filtration of water in test MGR15

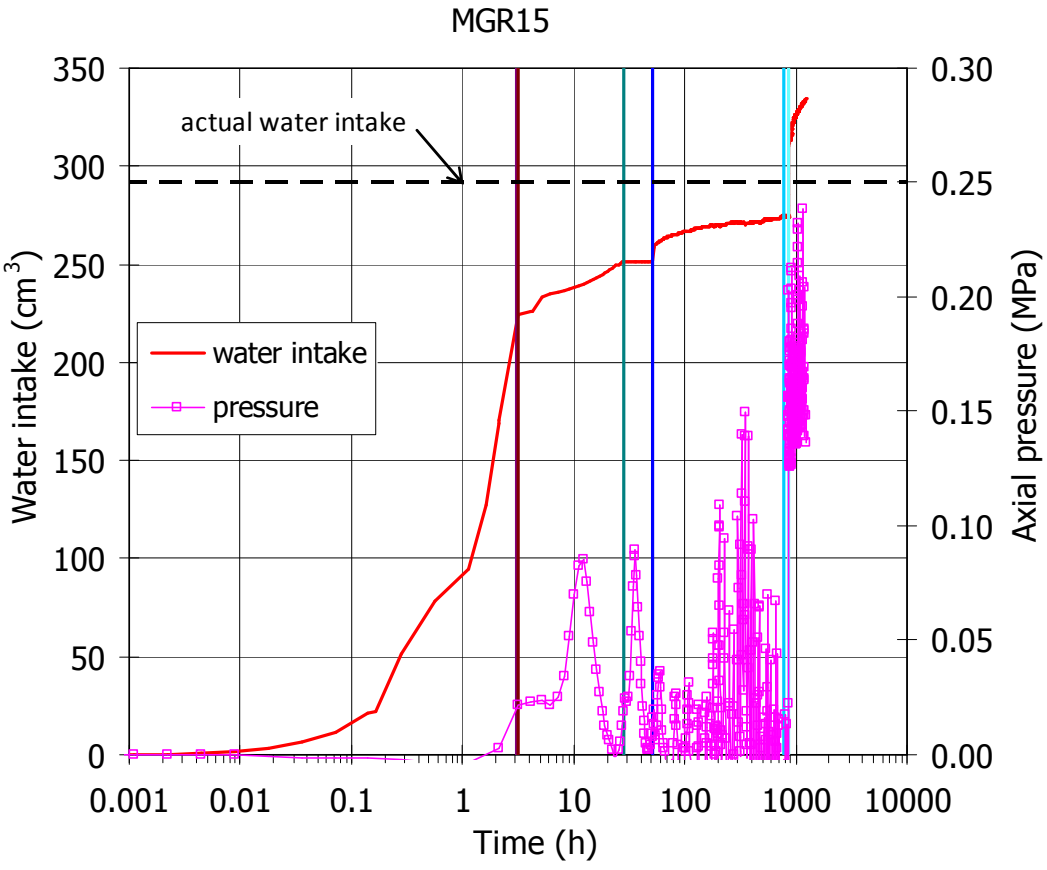


Figure 9: Evolution of water intake and axial swelling during test MGR15

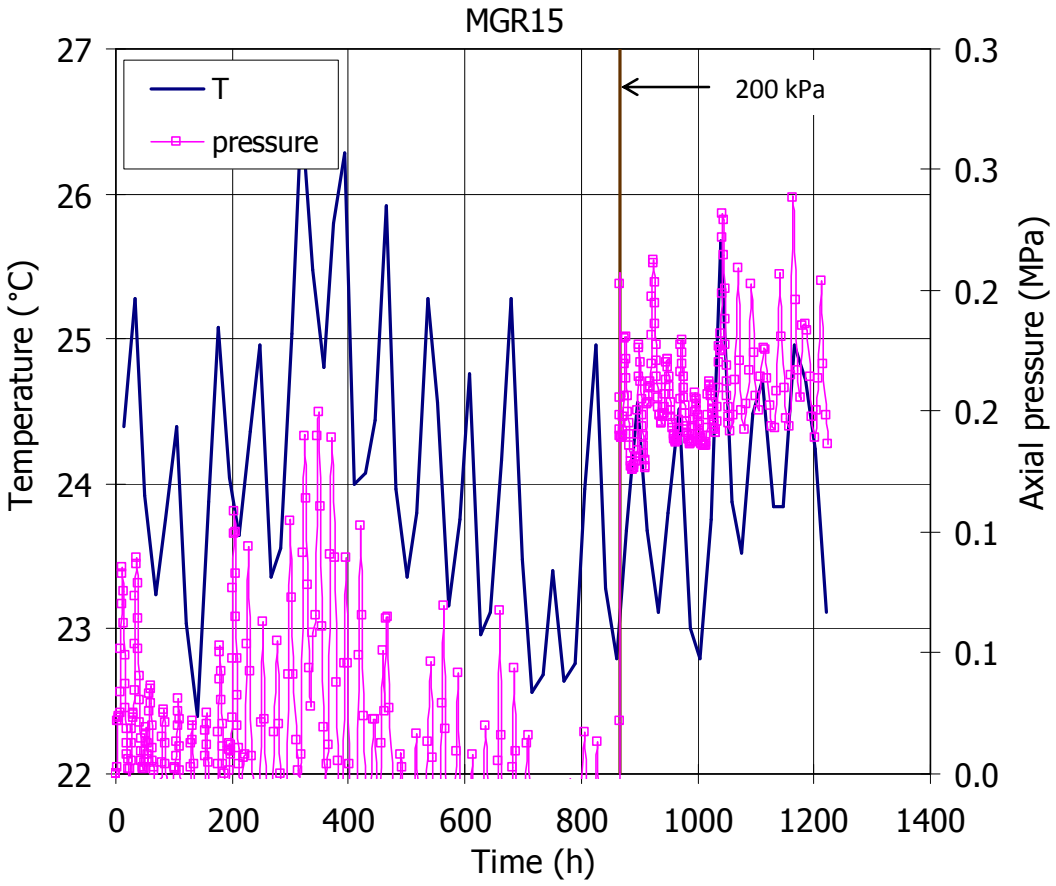


Figure 10: Evolution of axial pressure and temperature in test MGR15

4.1.1.2 POST MORTEM ANALYSES

After 51 days operation the cell was dismantled. The block was extracted, weighed and its dimensions measured. The block displayed a saturated appearance and was soft and easy to cut with a saw (Figure 11). It was cut in five sections in which only water content was determined, because the subsamples did not have enough consistency to determine dry density.



Figure 11: Appearance of sample MGR15 after extraction

From the final dimensions measurement the dry density of the block was 1.44 g/cm^3 and its final water content 29.9%, this would correspond to a degree of saturation of 92%. Figure 12 shows the measurements performed in the five equal levels in which the block was subsampled. The average water content from these measurements was 28.2%.

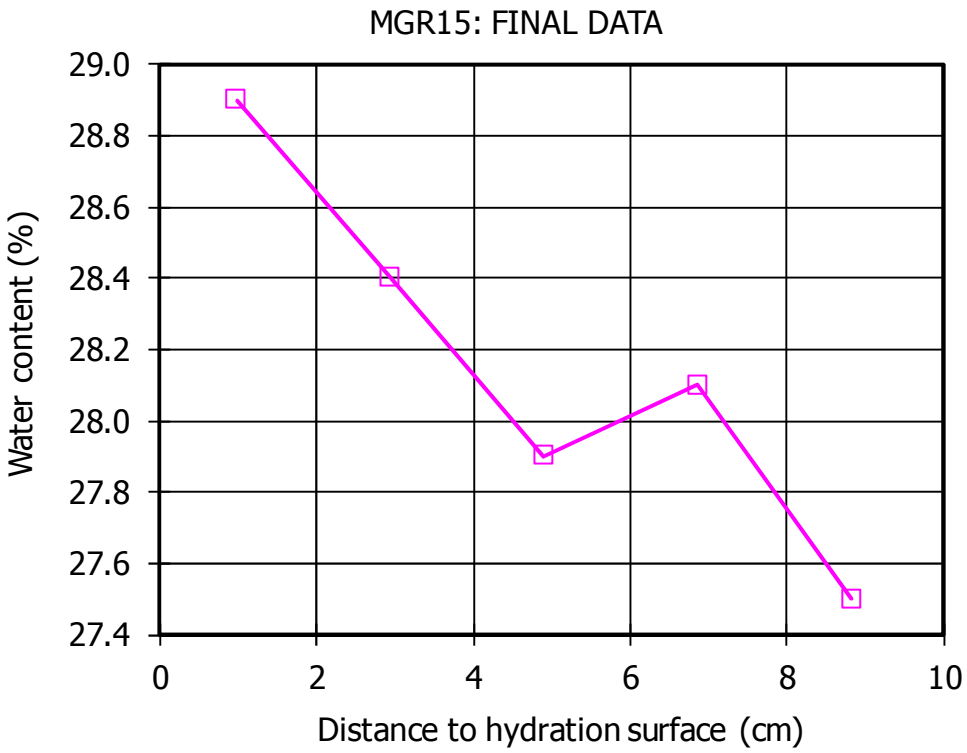


Figure 12: Final water content along the block MGR15

4.1.2 Test MGR16

A sample of the same characteristics as that used in test MGR15 was prepared, but the setup was modified in order to improve the measurements. Thus the load cell was changed by a 2-t one and the upper part of the sample was covered with a latex membrane and a copper plate to avoid water going out of the sample through it. The mixture was introduced inside the cell in spoonfuls and compacted beating with a hammer on the piston (Figure 13).



Figure 13: Appearance of the bottom part of sample MGR16 after compaction

4.1.2.1 ONLINE MEASUREMENTS

The test started in August 2011, using a 1.4 m water column to saturate the sample through the bottom. The water intake was very quick and the water deposit exhausted and had to be replaced a couple of times in the first hours. In addition, and despite the precautions taken, water was able to escape through the tube connected to the upper surface and the water inlet had to be kept closed for some time. Hence, the evolution of water intake as measured by the volume change apparatus shown in Figure 14 is overestimated. The actual water intake determined by final and initial weight difference of the sample is also shown in the Figure, which allows figuring out what the actual water intake rate could have been. The axial pressure developed during the test is also shown in the Figure, along with the previously mentioned events, which are indicated by thick vertical lines. Although the accuracy of the pressure measurement should have been higher than in test MGR15, due to the fact that a more suitable load cell was used, there was also a large dispersion in the measurements. The axial pressure was very low, on average 0.01 MPa, and greatly influenced by the temperature changes (Figure 15).

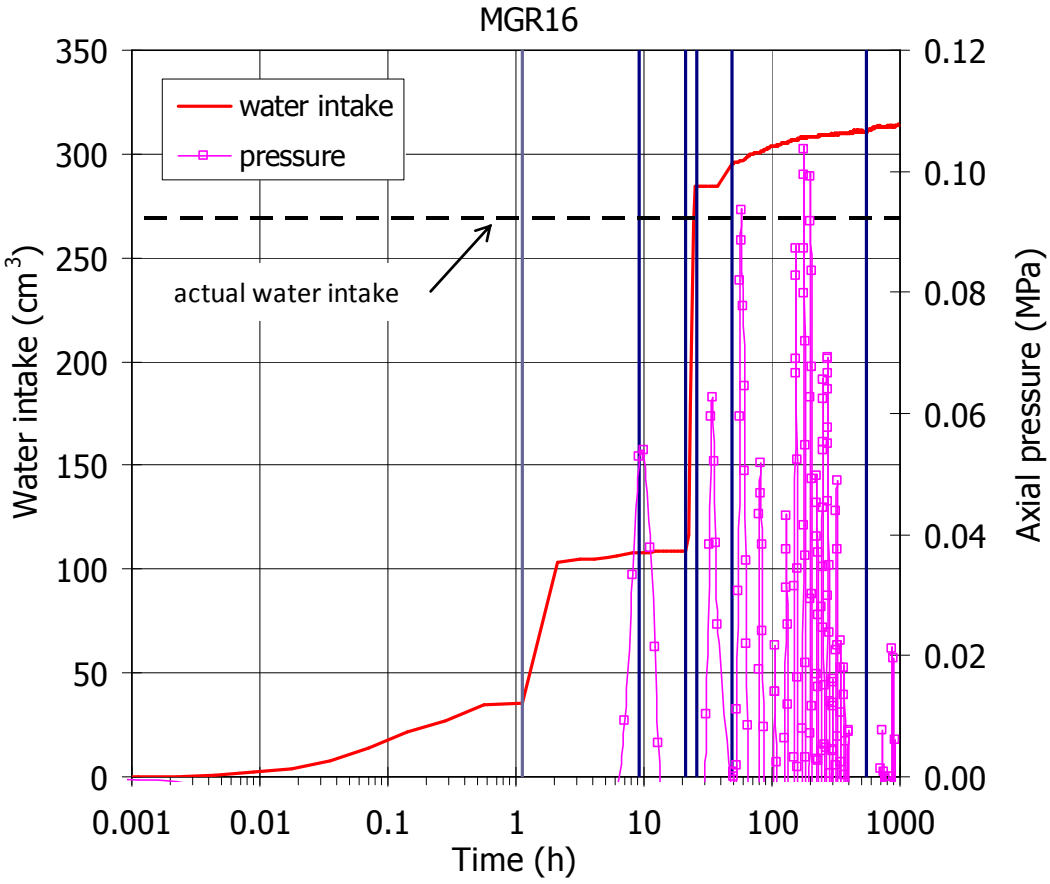


Figure 14: Water intake and axial pressure evolution during test MGR16

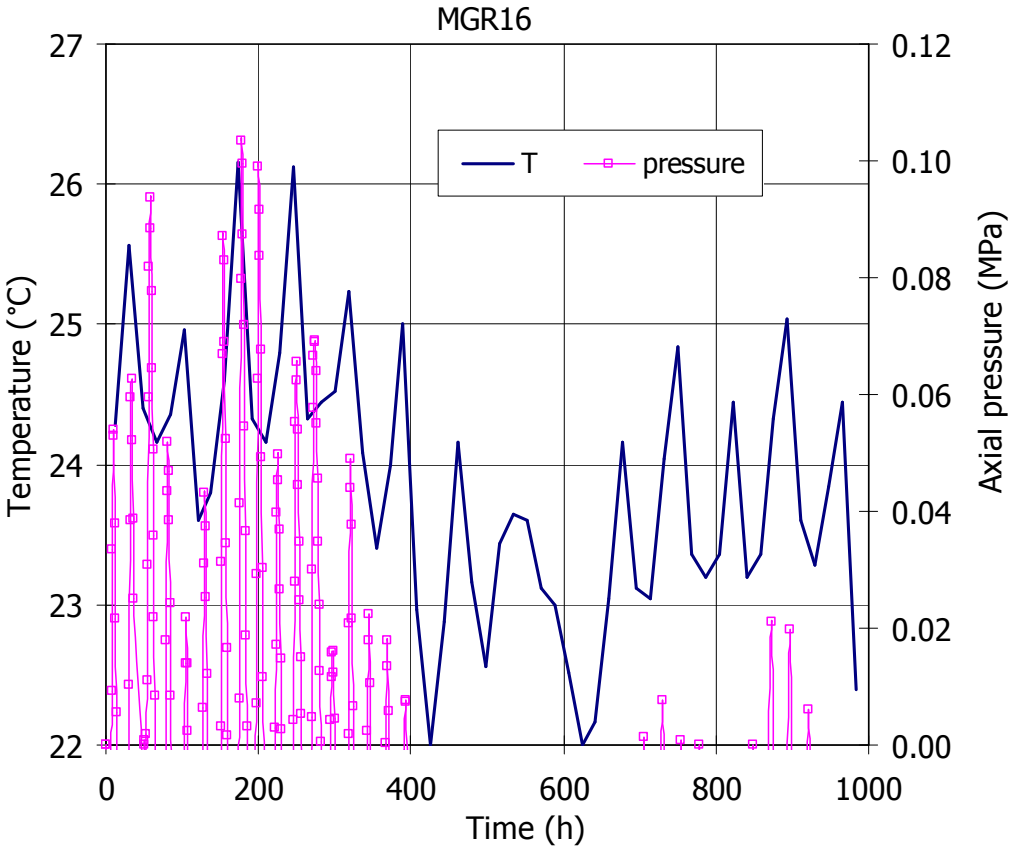


Figure 15: Evolution of axial pressure and temperature in test MGR16

4.1.2.2 POST MORTEM ANALYSES

After 41 days operation the oedometer cell was dismantled. The block was extracted and weighed. It was cut in four sections in which the water content was determined. The block displayed a saturated, homogeneous appearance (Figure 16) but the subsamples had not enough consistency to determine dry density in them. From the final and initial weight difference the final water content was 27.8%, which would correspond to a degree of saturation of 87%. Figure 17 shows the measurements performed in the four equal levels in which the block was subsampled. The average water content measured in the subsamples was 27.0%.

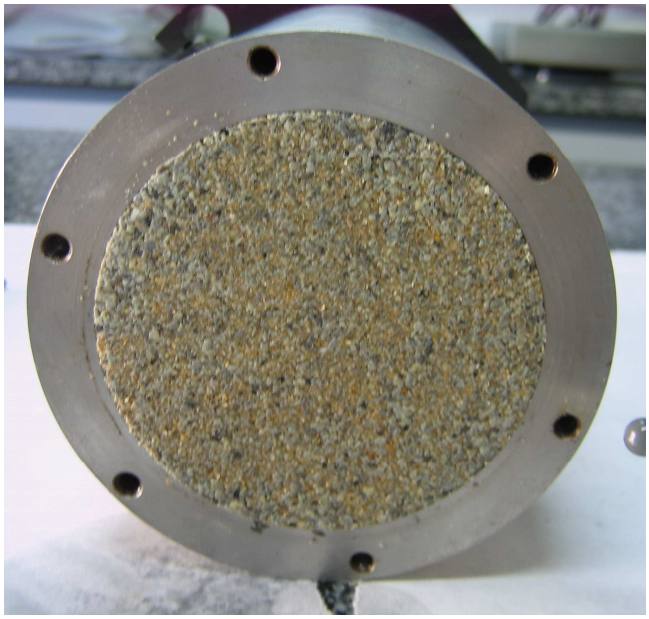


Figure 16: Final appearance of the sample from test MGR16

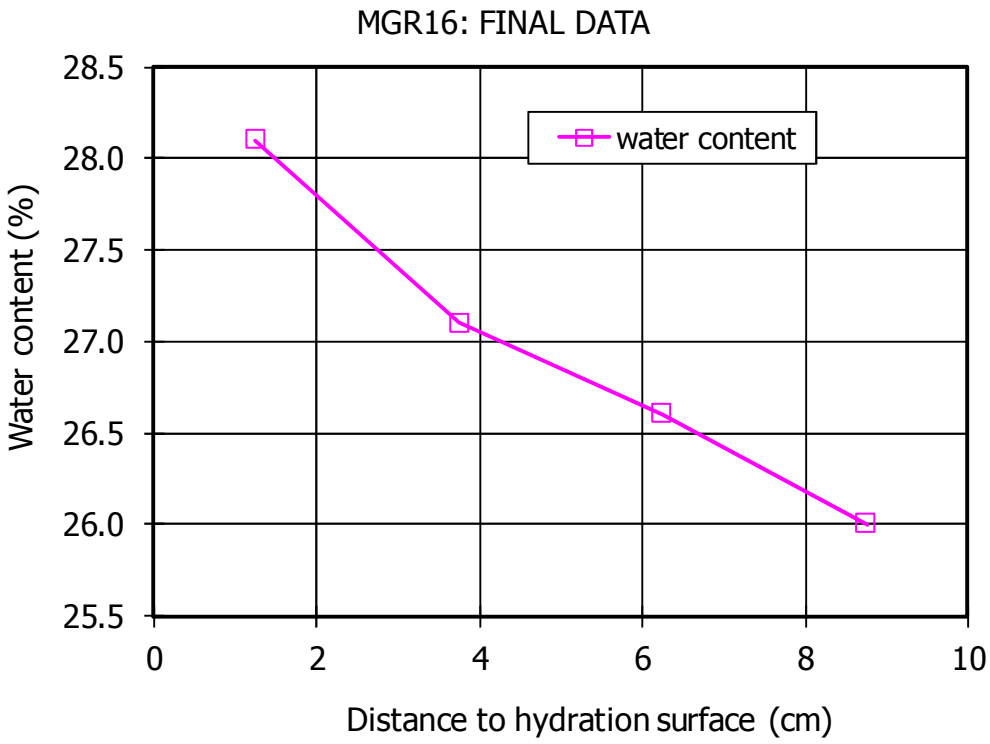


Figure 17: Final water content along the block MGR16

4.1.3 Test MGR19

Another test started with the same characteristics as the previous ones, with a 1.4-m water column as saturation pressure and the 2-t load cell. In this test the upper part of the sample was not sealed (Figure 18).

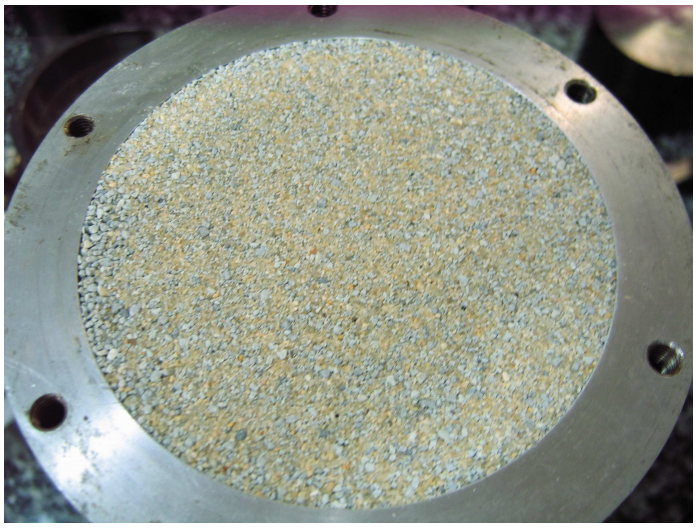


Figure 18: Appearance of the bottom part of sample MGR19 after compaction

4.1.3.1 Online measurements

The test started in May 2013. As in the previous tests the water deposit emptied several times and had to be replaced, for which reason the water intake stopped several times for short periods of time. After a few days the water injection pressure was increased to 300 kPa and later the tube connected to the upper surface of the sample was sealed to avoid water leaking through it. Nevertheless, water was able to pass between the cell wall and the piston and salt precipitated in the upper part of the oedometer (Figure 19). Hence, the evolution of water intake as measured by the volume change apparatus shown in Figure 20 is overestimated. Taking into account the final weight of the sample (which as explained in the next section is also uncertain), the range of actual water intake is indicated in the Figure. Although the span of this range is as large as 50 cm^3, it is in any case well below the measurement of the volume change apparatus. The water injection pressure was further increased to 400 kPa, which was immediately recorded by the load cell. The axial pressure developed during the test is also shown in the Figure, along with the previously mentioned events, which are indicated by thick vertical lines. It can be observed that during the phase in which the water injection pressure was very low, the load cell did not record any pressure above the initial one set to fix the cell in the oedometer frame.

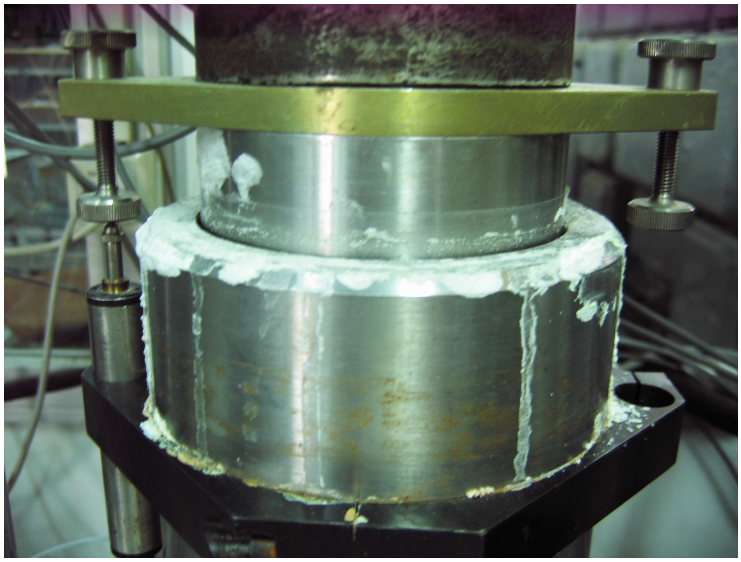


Figure 19: Salt precipitates in the upper part of the oedometer due to water leaking along the cell wall

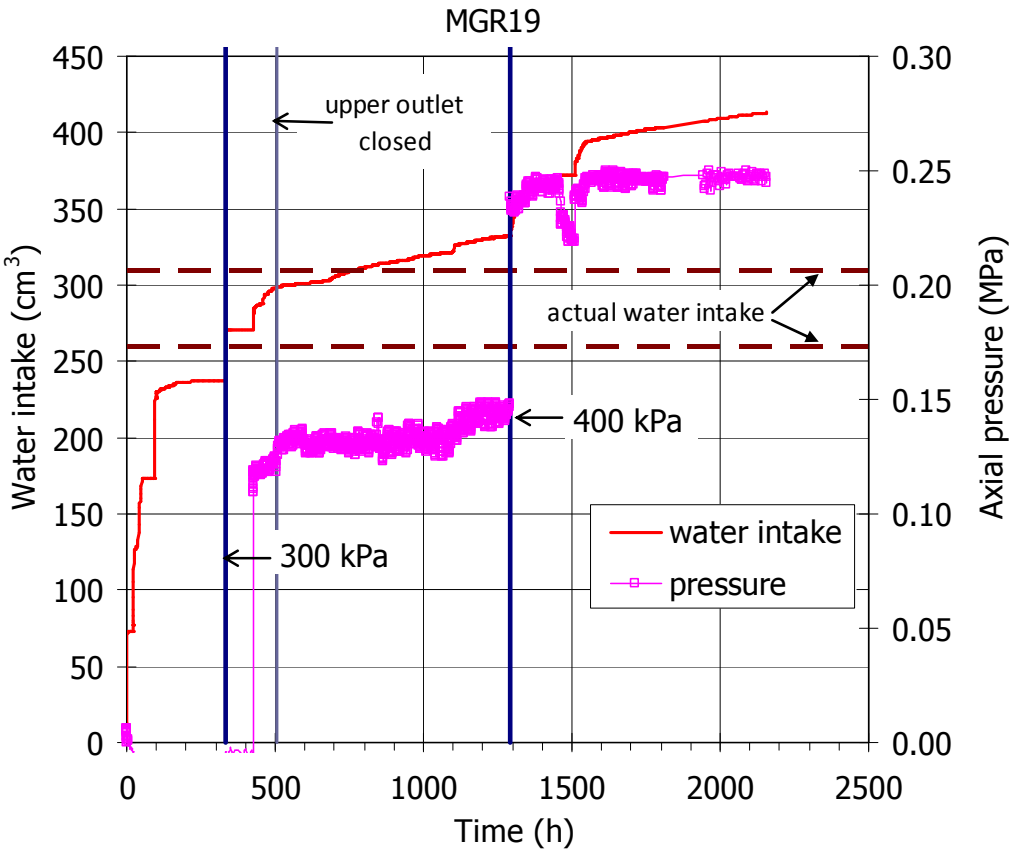


Figure 20: Water intake and axial pressure evolution during test MGR19. The uncertainty in the actual water intake is indicated by two thick horizontal lines

4.1.3.2 POST MORTEM ANALYSES

After 144 days operation the oedometer cell was dismantled. Due to a wrong manipulation during dismantling the sample was flooded and it lost its consistency. As a consequence the final dry density could not be determined. The average water content measured in the subsamples was 31.5%, which would correspond to a 100% degree of saturation, but this reflects the massive water entrance upon dismantling, which could be as high as 50 cm^3.

4.2 TESTS WITH BENTONITE PELLETS

4.2.1 Test MGR17

The bentonite pellets were placed inside the cell in spoonfuls and the target dry density was reached by applying a slight uniaxial pressure. The upper part of the oedometer was sealed with a latex membrane, in order to avoid water going out of the cell through the upper surface of the sample. A 1.4-m column was used to apply the water pressure at the bottom surface and a 2-t load cell was used to measure the vertical pressure developed upon saturation.

4.2.1.1 ONLINE MEASUREMENTS

The test started in October 2011 and was dismantled in February 2012, the total duration being 118 days. The evolution of water intake as measured by the volume change apparatus along with the axial pressure developed during the test are shown in Figure 21. After approximately 95 days the axial pressure reached the maximum value allowed by the load cell and it had to be replaced. For that, the axial load had to be released and the cell taken out of the oedometer frame for about three hours. During this time the cell was confined in a different frame in order to avoid the expansion of the sample. When moved again to the oedometer frame, the deformation of the sample was adjusted to that before removing the axial load. However, it was not possible to relate the new values recorded to those previous to the load cell replacement (Figure 22) for which reason they are not considered reliable. Thus, it can only be said that the final swelling pressure was higher than 2.5 MPa (Figure 21).

At the end of the test the water content according to the volume change apparatus would be 28.2%, which is very close to that checked upon dismantling by final and initial weight difference, which was 28.4%.

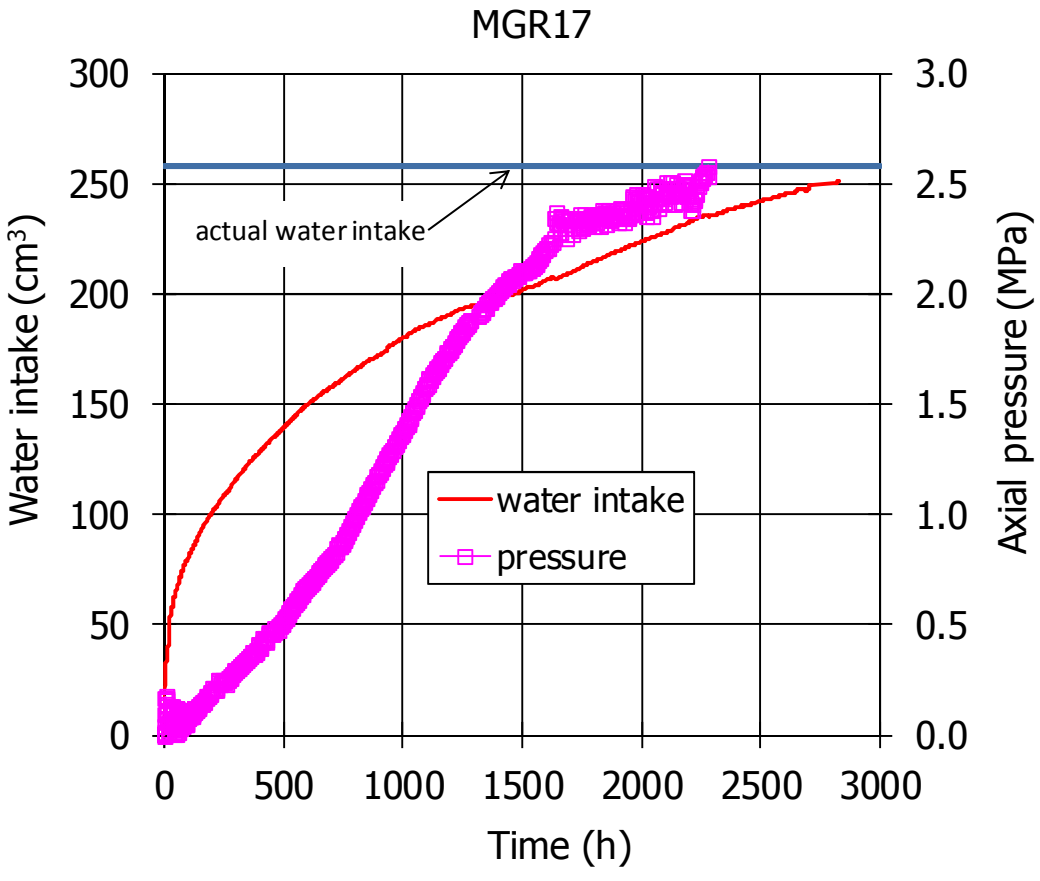


Figure 21: Water intake and axial pressure evolution during test MGR17

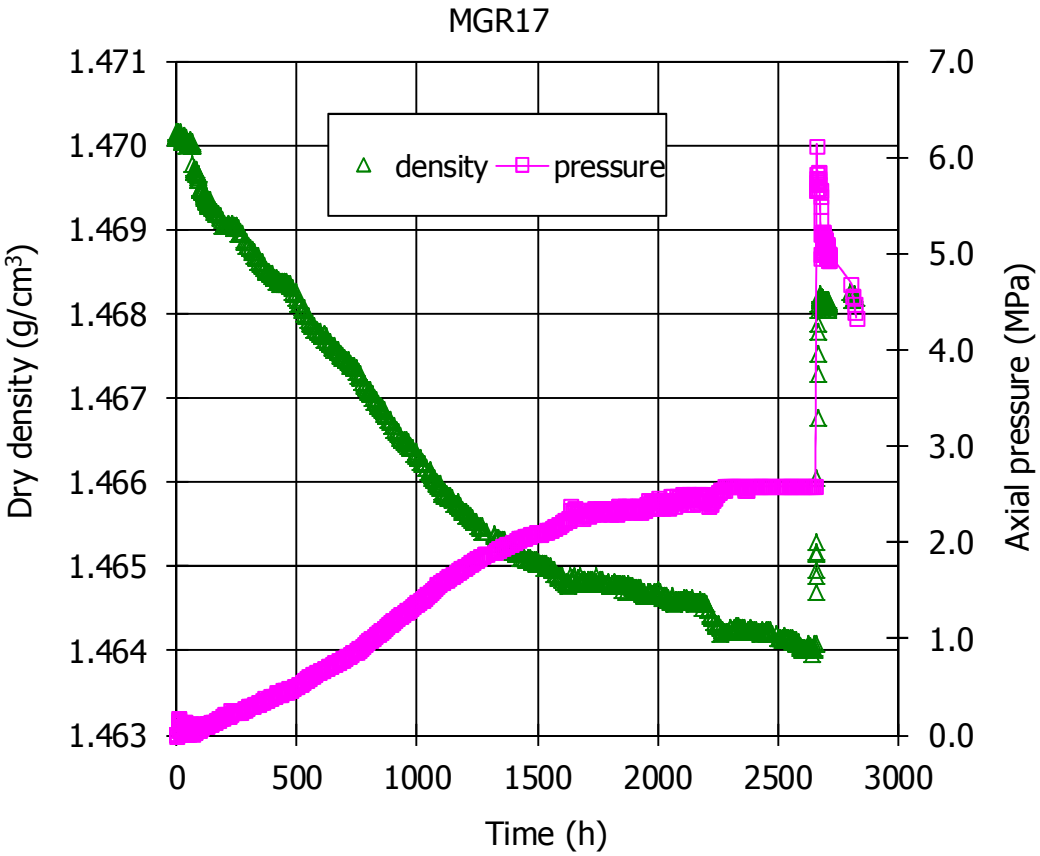


Figure 22: Dry density and axial pressure evolution during test MGR17 (the sharp changes correspond to the change of load cell)

4.2.1.2 POST MORTEM ANALYSES

After 118 days operation the oedometer cell was dismantled. The block was extracted, weighed and its dimensions measured. It looked homogeneous and was consistent, although there was a clear difference between the bottom and upper surfaces (Figure 23). In the latter one pellets could be still identified. It was cut in five sections in which dry density and water content were determined (Figure 24).

From the final dimensions and weight measurement the dry density of the block was 1.53 g/cm^3 and its final water content 28.4%, this would correspond to a degree of saturation of 97%. Figure 25 shows the measurements performed in the five levels in which the block was subsampled. The average water content measured in the subsamples was 28.3% and the dry density was 1.54 g/cm^3. The water content and dry density gradients along the sample were significant.

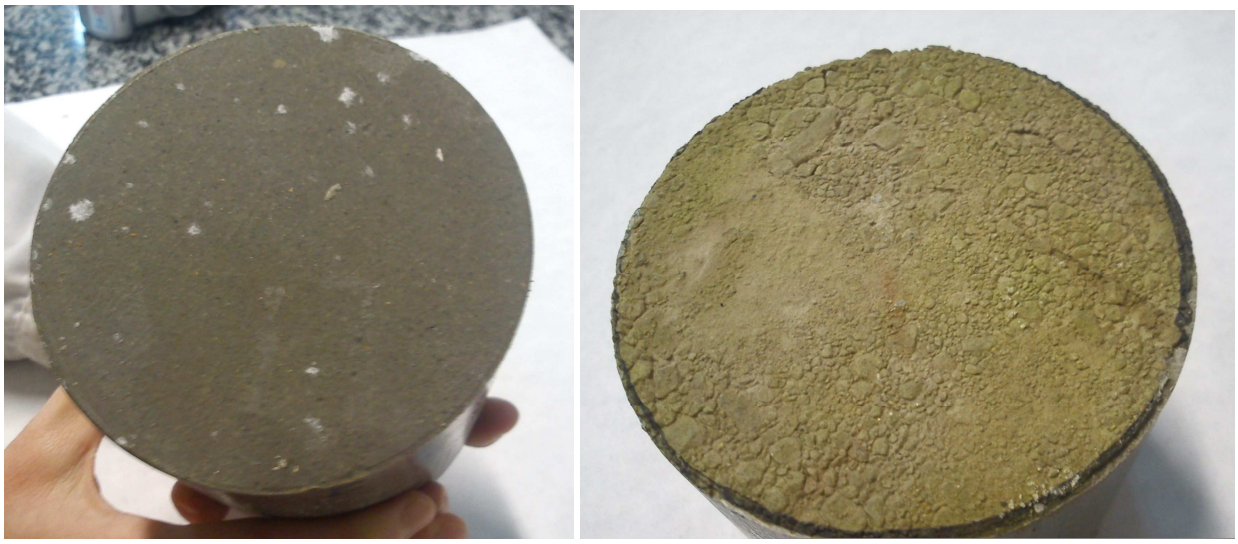


Figure 23: Final appearance of the bottom (left) and upper (right) surface of sample from test MGR17



Figure 24: Subsampling sections for sample MGR17 and internal appearance after longitudinal cutting

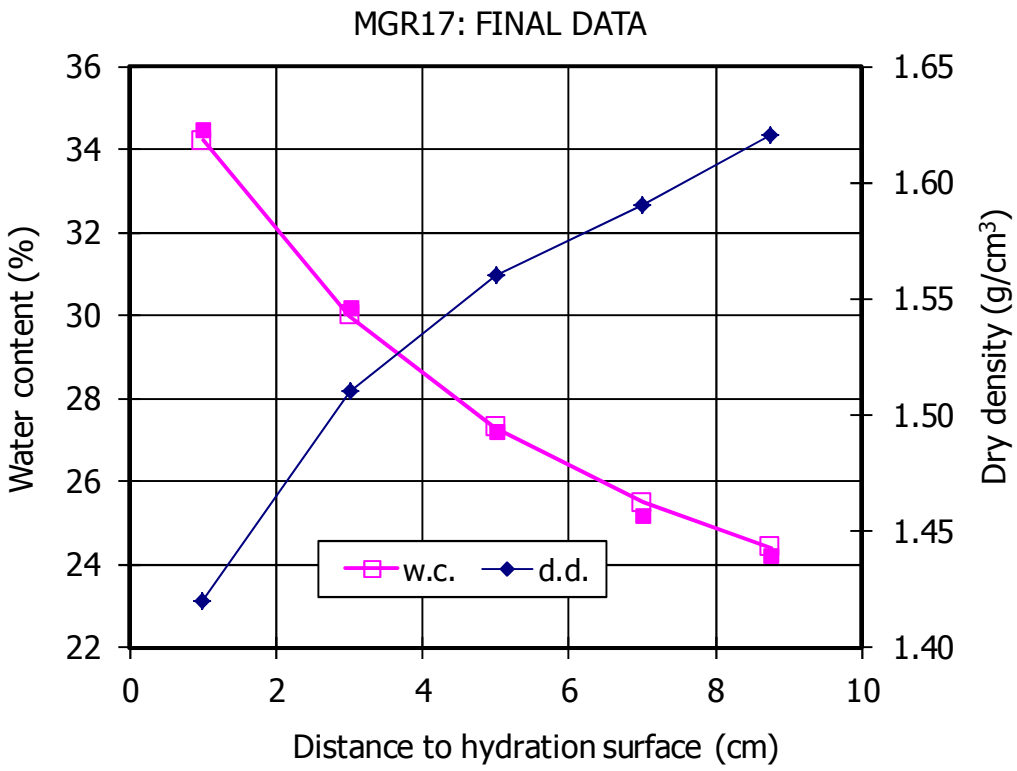


Figure 25: Final water content (w.c.) and dry density (d.d.) along the block MGR17

4.2.2 Test MGR18

This test was set as test MGR17: the bentonite pellets were placed inside the cell in spoonfuls and the target dry density was reached by applying a slight uniaxial pressure. The upper part of the oedometer was not sealed though. A 1.4-m column was used to apply the water pressure at the bottom surface and the 10-t load cell was used to measure the vertical pressure developed upon saturation.

4.2.2.1 Online measurements

The test started in February 2012 and was dismantled in April 2013, the total duration being 446 days. The evolution of water intake as measured by the volume change apparatus along with the axial pressure developed during the test are shown in Figure 26. The water injection pressure was increased twice during the test, first to 0.2 MPa and finally to 0.6 MPa. These increases were not reflected in the axial pressure measurements, but they meant an increase of the water intake rate. The final axial pressure value was 6.6 MPa, which is above the value obtained with Equation 1 for small MX-80 samples of dry density 1.57 g/cm^3 saturated with deionised water (5.0 MPa). This dry density, higher than the nominal initial one, was deduced from the final dimensions of the bentonite block obtained upon dismantling.

At the end of the test the water content according to the volume change apparatus would be 27.7%, which is slightly above that checked upon dismantling by final and initial weight difference, which was 27.2%. In fact, the water intake after increasing the injection pressure to 0.6 MPa seems overestimated. Since the upper surface of the sample was opened to atmosphere, some evaporation could have taken place through it.

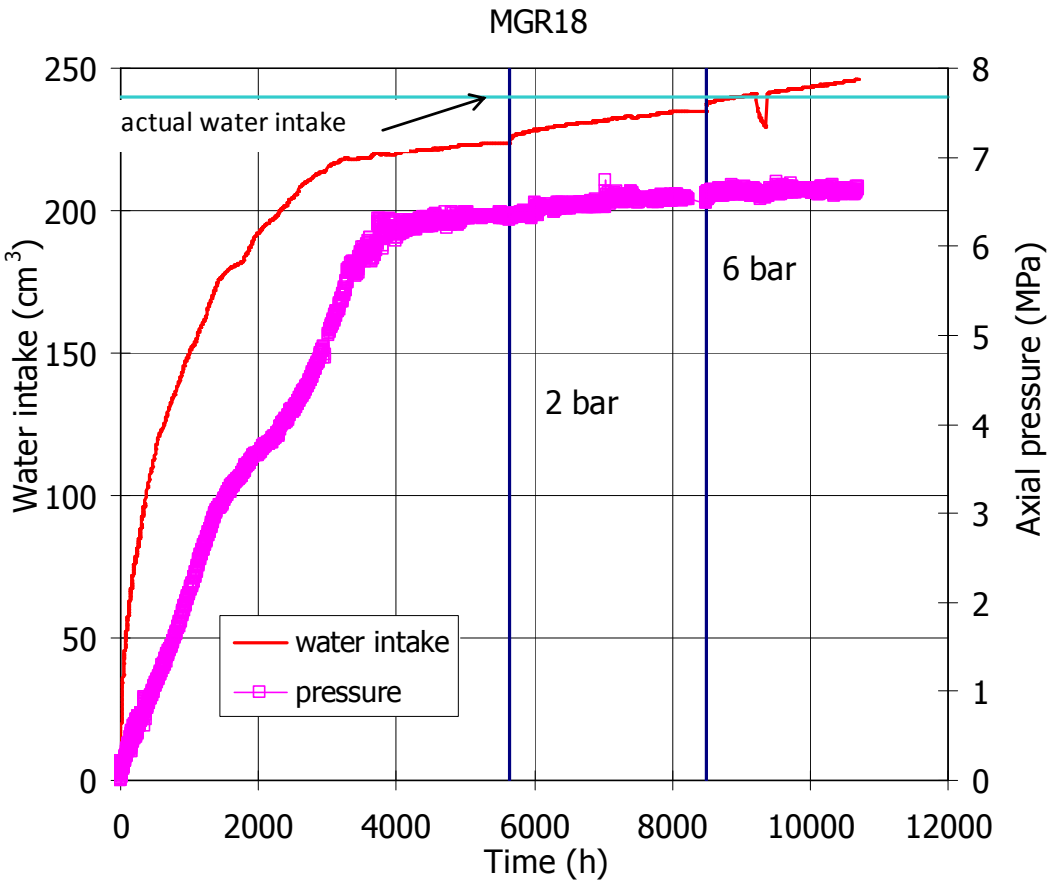


Figure 26: Water intake and axial pressure evolution during test MGR18 (the thick vertical lines indicate the increase in water injection pressure)

4.2.2.2 POST MORTEM ANALYSES

After 446 days operation the oedometer cell was dismantled. The block was extracted, weighed and its dimensions measured. It was consistent and looked homogeneous, no pellets could be identified (Figure 27). It was cut in four sampling sections in which dry density and water content were determined.

From the final dimensions and weight measurement the dry density of the block was 1.57 g/cm^3 and its final water content 27.2%, this would correspond to a degree of saturation of 100%. Figure 28 shows the measurements performed in the four levels in which the block was subsampled. The average water content measured in the subsamples was 27.0% and the dry density was 1.58 g/cm^3. The water content and dry density gradients along the sample were significant in the 6 cm closest to the hydration surface.



Figure 27: Final appearance of the bottom surface and subsampling sections of sample from test MGR18

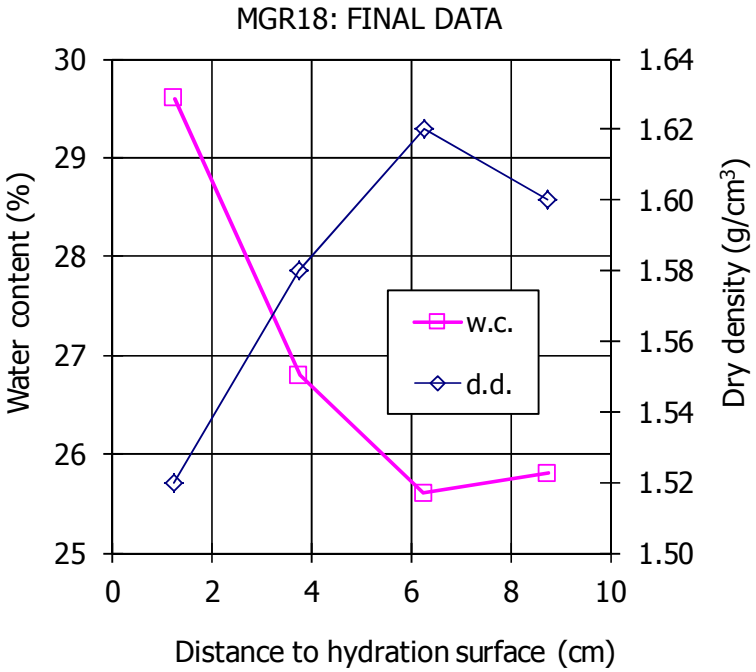


Figure 28: Final water content (w.c.) and dry density (d.d.) along the block MGR18

For the mercury intrusion porosimetry (MIP) tests the subsamples were lyophilised 6 days after dismantling and analysed 17 days later. Figure 29 shows the corrected (taking into account the pore volume not intruded by mercury) incremental pore volume for the samples tested, with sample 4 being the closest to the hydration surface. The curve for the original material (dry pellets mixture) is also plotted in the Figure. The percentage of the porosity intruded by the mercury in the samples from test MGR18 was between 50 and 60%, this meaning that there was an important volume of pores with a size of less than 7 nm or not interconnected, which have been considered micropores. Figure 30 and Table III show the pore size percentages recalculated and the mode of each pore size. In addition to the predominance of the micropore size, it can be observed that the size of the macropores decreased towards the hydration surface. This macropore family developed upon hydration, since it did not appear in the original sample, which probably had a macropore size too large to be detected by MIP (larger than 500 µm).

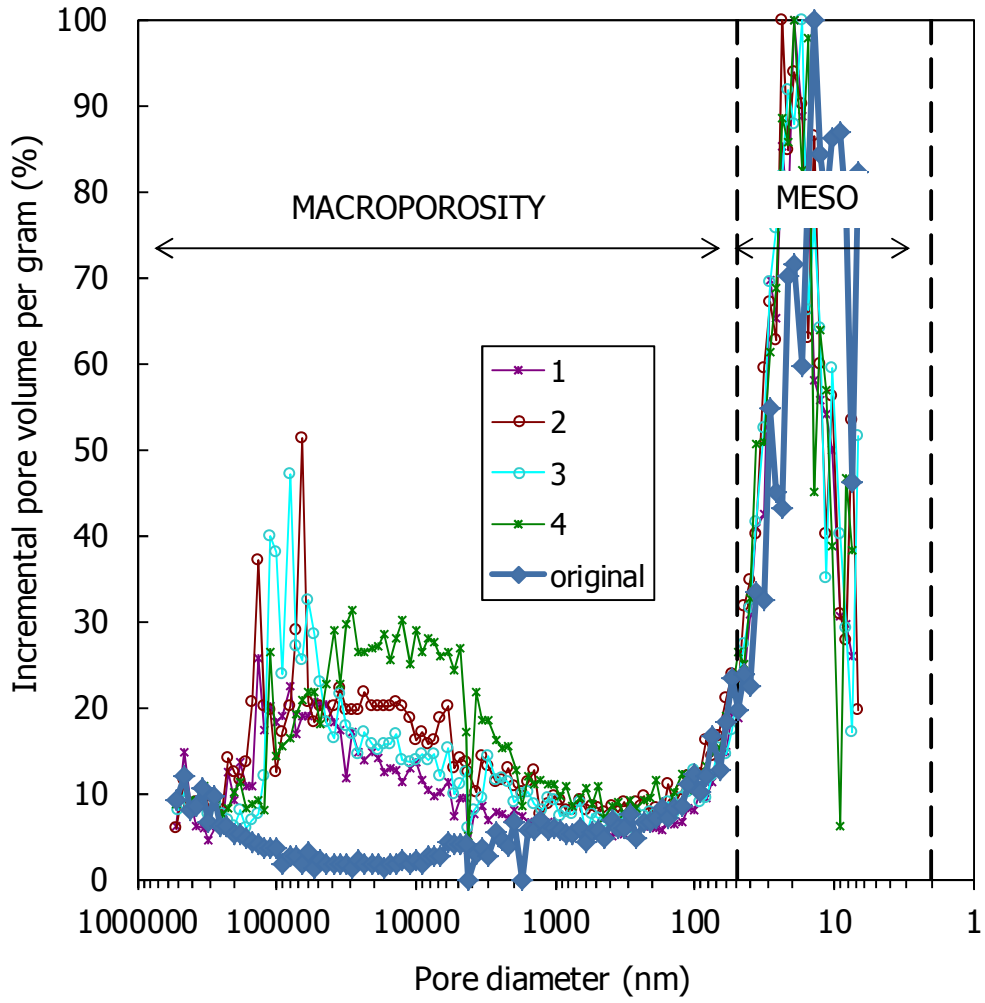


Figure 29: Mercury intrusion porosimetry results for samples of test MGR18 (sample 4 is the closest to the hydration surface)

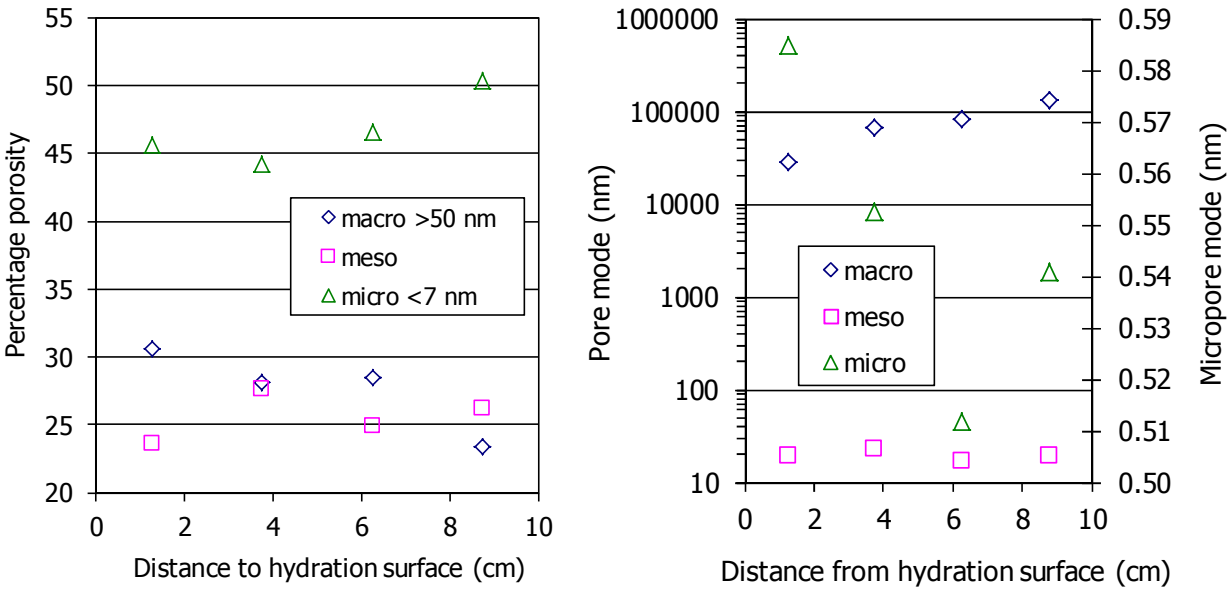


Figure 30: Pore size distribution and pore mode of samples from test MGR18 (the micropore mode was obtained from the basal spacing measured by X-ray diffraction)

Table III: Final characteristics of samples from test MGR18, including MIP and X-ray diffraction results (sample 4 is the closest to the hydration surface)

Sample	ρ_d (g/cm^3)	*w* (%)	% intruded	% macro	Mode macro (nm)	% meso	Mode meso (nm)	% micro	*d*(001) (nm)
1	1.60	25.7	50	23	134692	26	19	50	1.521
2	1.62	25.6	53	29	81004	25	17	47	1.492
3	1.58	26.7	56	28	65890	28	23	44	1.532
4	1.52	29.4	54	31	28529	24	19	46	1.565

Figure 31 shows the X-ray diffraction patterns obtained for the 4 subsamples of the block. These analyses were performed immediately after dismantling. From these diffraction patterns the basal spacing of the smectite could be determined, and the values obtained are included in Table III (*d*(001)). The peak indicating the basal spacing was in the four samples a double one, and the two peaks could be told apart by profile fitting of the XRD pattern. An example of this fitting is shown in Figure 32 (Gutiérrez-Nebot 2013). For the more intense peak in each sample an average value of 1.53 nm, corresponding to a 2-water layer hydration state, was obtained. Taking into account that these values correspond to the joint thickness of the TOT layer and of the interlayer, a micropore size was computed by subtracting to the basal spacing value the thickness of the TOT layer (assumed 0.98 nm) and the values obtained are those plotted in Figure 30.

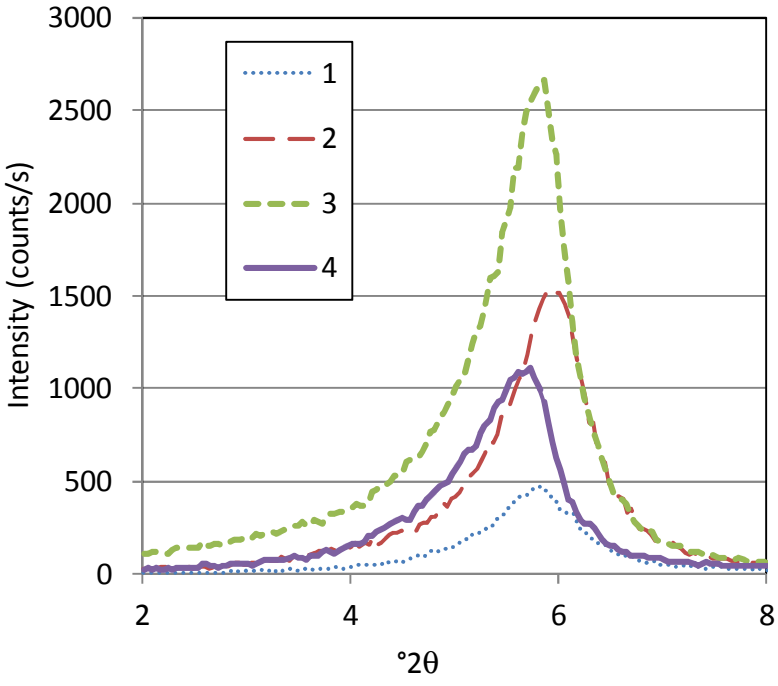


Figure 31: X-ray diffraction patterns of untreated samples from test MGR18 (sample 4 is the closest to the hydration surface)

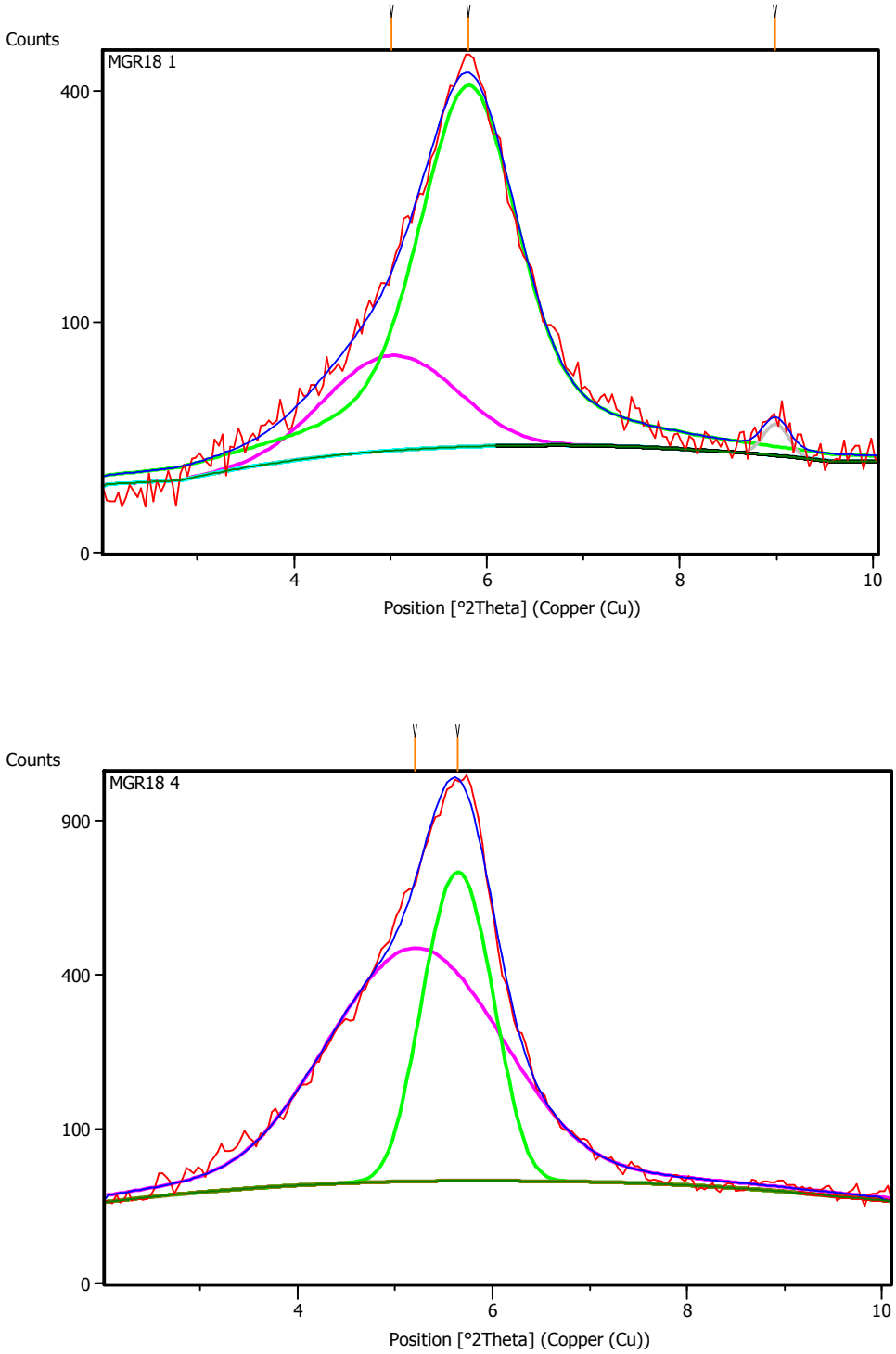


Figure 32: Profile fitting of the XRD pattern of samples MGR18-1 (up) and 4 (down). Sample 4 is the closest to the hydration surface (Gutiérrez-Nebot 2013)

5 Summary and conclusions

Five saturation tests under isochoric conditions were performed in a large oedometer with the materials used in the Mont Terri *in situ* HE-E experiment, three of them with the sand/bentonite mixture (S/B) and two with the bentonite pellets (B). The bentonite was the MX-80. The nominal length and diameter of the samples was 10 cm. The nominal dry density of the mixtures was low as well as the water content, for which reason it was not necessary to

apply high compaction pressures to prepare the tests samples. Pearson synthetic water was used to saturate the specimens, as in the *in situ* test. The water intake and the vertical stress developed upon saturation as well as the small vertical deformation allowed were measured. After dismantling, water content and dry density were determined along the specimens and in test MGR18 other post mortem determinations related to the analysis of the bentonite microstructure were performed.

The sand/bentonite mixture did not develop any significant swelling upon saturation (or it was too low to be detected with accuracy by the load cells used). According to the results obtained in small oedometers, the expected swelling pressure would be 0.7 MPa. Figure 33 shows the online measurements of the three tests performed with the S/B mixture. Most of the water intake took place at the beginning of the tests, in fact, in three hours of water injection under a very low pressure, water went through the 10-cm long sample and out of the cell. The subsequent increases of water injection pressure were quickly reflected by the load cell, but they do not seem to have implied an acceleration of the saturation rate, but just a higher leakage through the opposite surface. Despite the high water intake rate, full saturation and homogeneous water content had not been reached after 51 days (Figure 34).

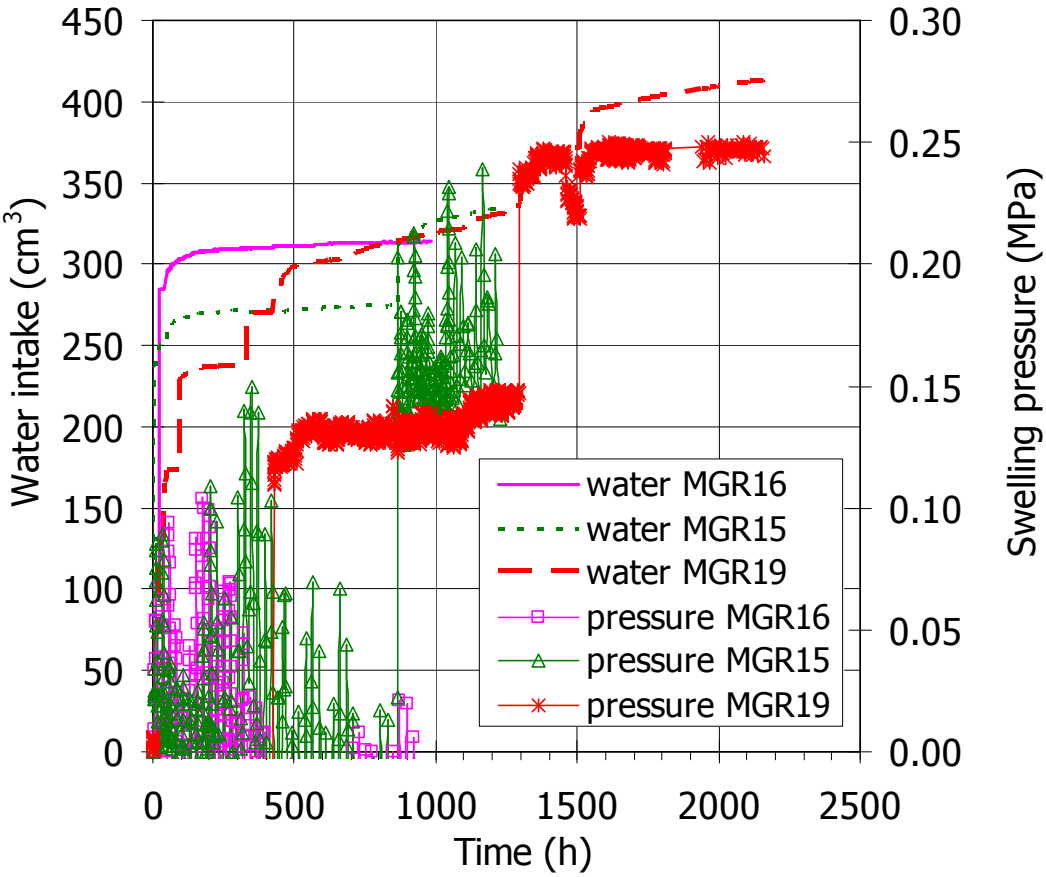


Figure 33: Evolution of swelling pressure and water intake in the tests performed with the S/B mixture

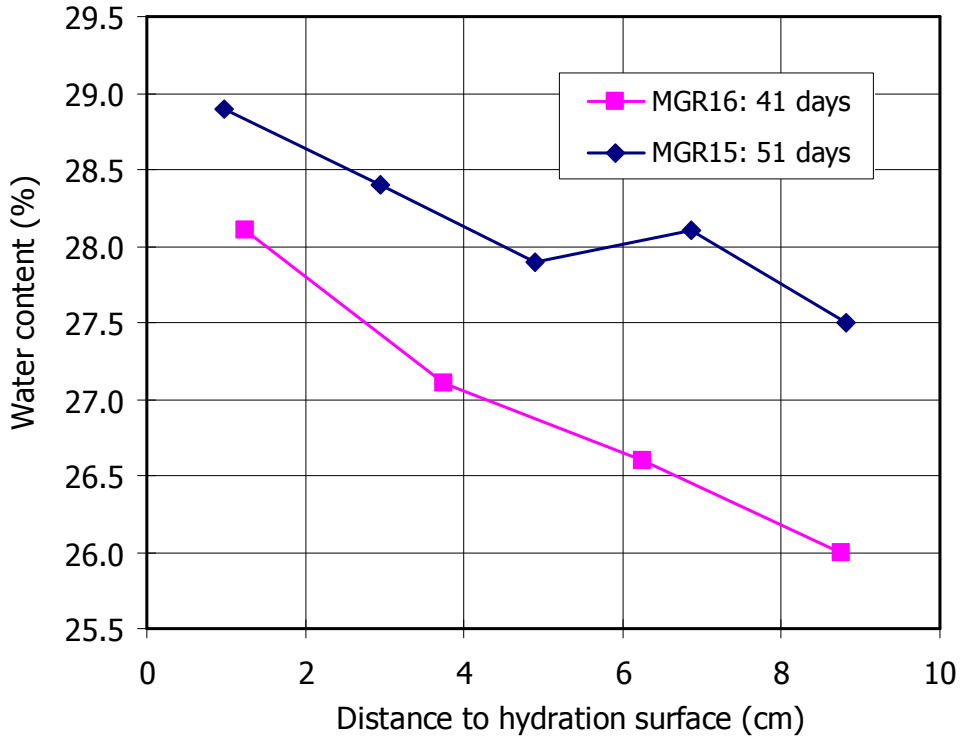


Figure 34: Final water content along the S/B mixture columns

Figure 35 shows the evolution of water intake and axial pressure in the two tests performed with the pellets mixture. The dry density checked at the end of the tests was higher than the target one: 1.53 g/cm^3 (MGR17) and 1.57 g/cm^3 (MGR18) instead of 1.47 g/cm^3. This deviation originated probably at the beginning of the tests, when the cell was placed in the oedometric frame and a small initial axial pressure was applied. Since the material had a very low dry density this pressure could have caused the increase in dry density. The measurement of axial pressure in test MGR17 stopped before the end of the test, thus the final value recorded does not correspond to the equilibrium value for the final water content. It was clear that most of the water was taken at the beginning of the experiments, when the axial pressure development was also sharper.

Previous experience from tests performed in similar oedometers with bentonite showed that the development of swelling pressure followed systematically a pattern in which the pressure increased sharply at the beginning of hydration, then stabilised or slightly decreased, and afterwards increased again, eventually reaching the equilibrium value. This was the pattern observed in the two tests performed with bentonite pellets. The following conclusions concerning swelling pressure development in bentonites were drawn (Imbert & Villar 2006):

1 The increase/decrease/increase pattern of swelling pressure development appeared irrespective of dry density, size of sample and fabric.

2 The kinetics of the process depended on dry density, initial water content and size of the sample. This last fact should be taken into account when transferring laboratory test results to field conditions where scale and hydration paths are bound to be quite different (Gens *et al*. 2011).

3 The mixtures became homogeneous upon saturation, with swelling pressure and hydraulic conductivity similar to those of compacted powder of the same dry density.

4 Scale effect: the swelling pressure obtained in large oedometers tended to be higher.

The final swelling pressure values have been plotted in Figure 36 as a function of the final dry density checked by measurement of the dimensions of the samples upon dismantling. The results and empirical fitting for the swelling pressure of MX-80 powder bentonite obtained in small standard oedometers is also included in the Figure (Equation 1). The vale obtained in test MGR18 is higher than the theoretical value obtained with the empirical fitting, despite the fact that Pearson water was used in this test and deionised water was used in the tests from which the fitting was derived. However, salinity is considered to reduce smectite swelling pressure, specially when it is compacted to low dry densities. In fact, Karnland et al. (2005) measured reductions of the swelling pressure of MX-80 bentonite with the salinity of the saturating fluid, which were relatively lower as the clay density was higher. As mentioned above, the swelling pressure tended to be higher when it was determined in large samples, which is another factor that could contribute to this high swelling pressure value. The value obtained in test MGR18 does not correspond to a saturated sample, hence it is a minimum value.

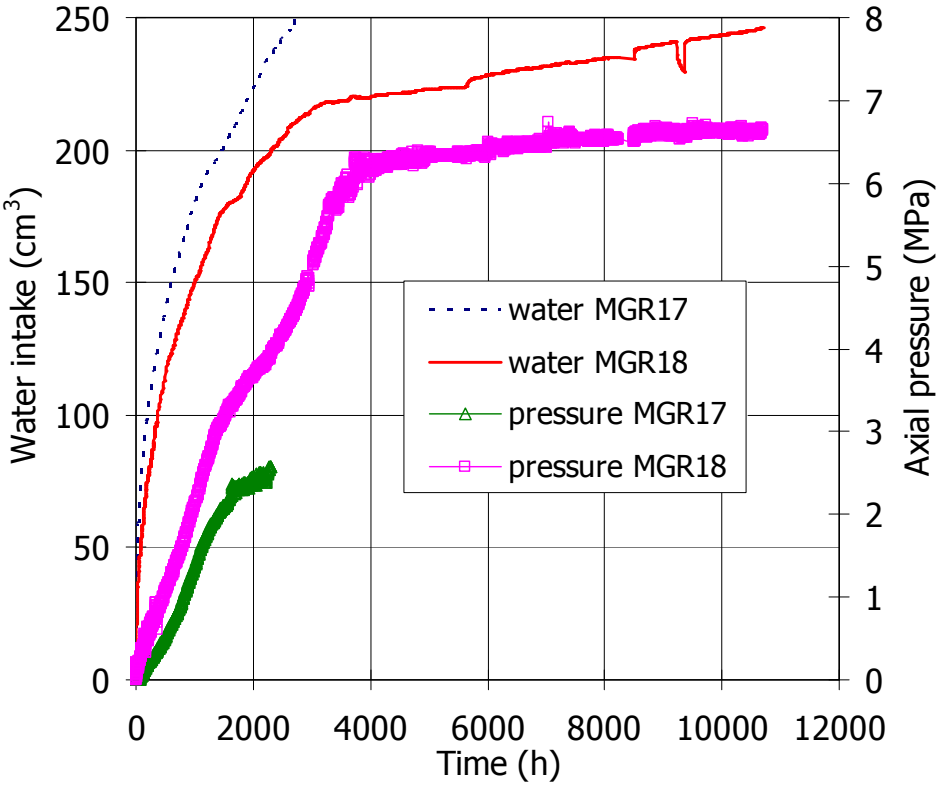


Figure 35: Evolution of swelling pressure and water intake in tests MGR17 and MGR18 (bentonite pellets)

Upon dismantling the water content and dry density along the blocks was checked (Figure 37). There was a clear gradient for both properties in the two tests, sharper in the shorter test MGR17. It is significant that the gradients remained in test MGR18, despite the fact that an equilibrium swelling pressure value had been reached.

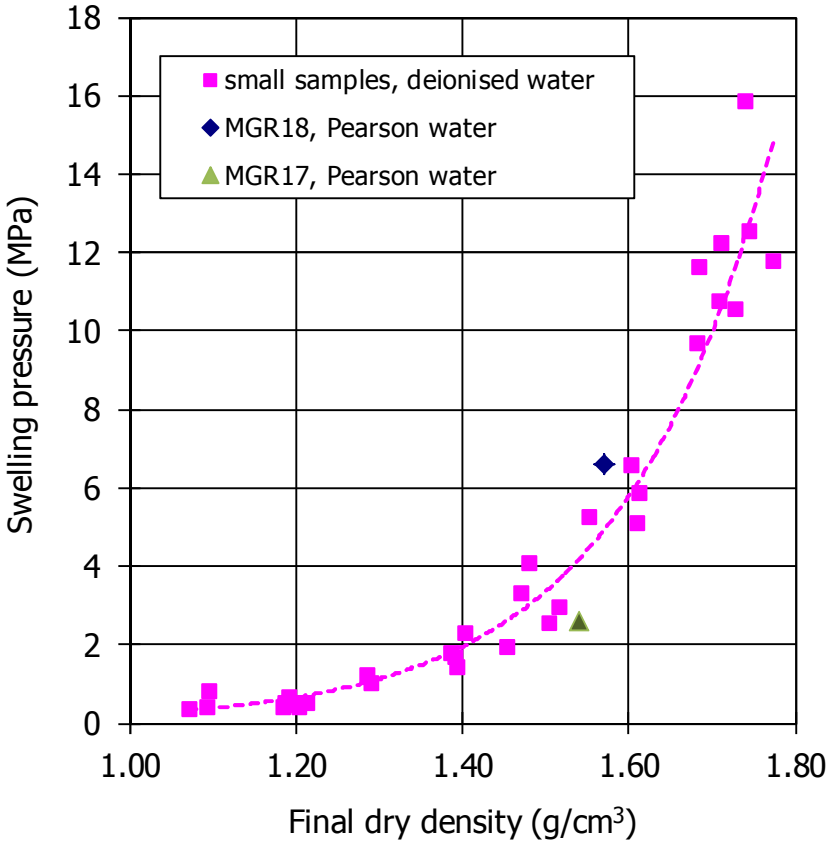


Figure 36: Swelling pressure values measured in the tests performed in the large oedometer and results and empirical fitting for MX-80 bentonite powder (Equation 1). The result for test MGR17 is a minimum value

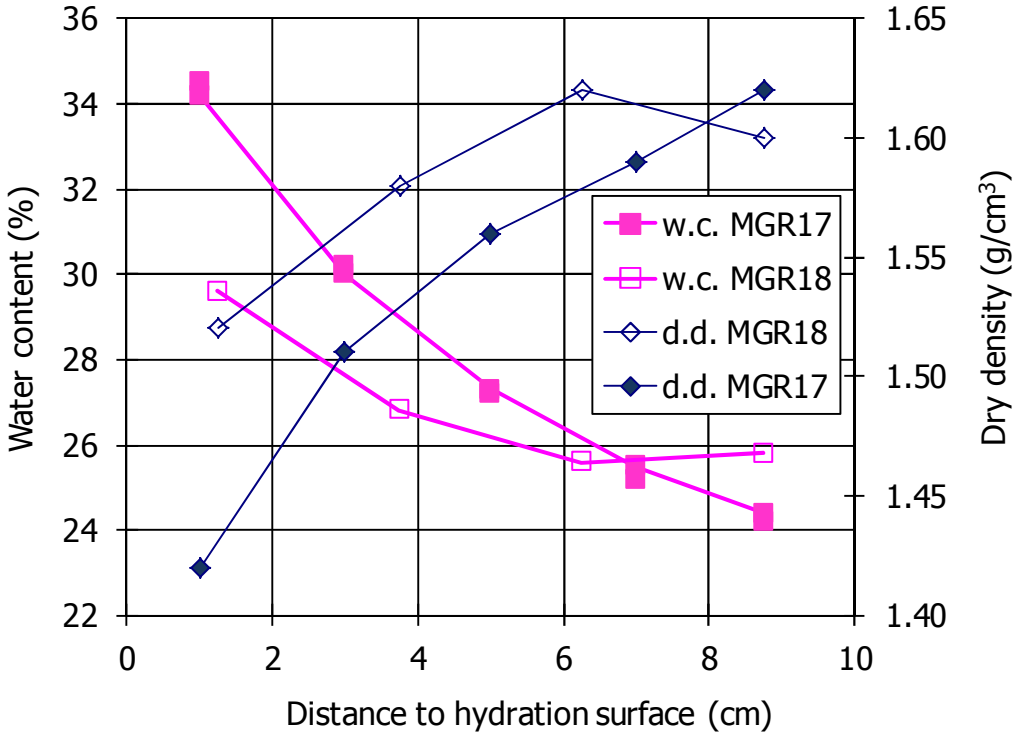


Figure 37: Final dry density (d.d.) and water content (w.c.) along the bentonite columns

The pore size distribution obtained by MIP in test MGR18 showed that the micropore size (diameter <7 nm) is the predominat one after saturation. Since the micropore size cannot be explored with the MIP technique, the measurement of the basal spacing by X-ray diffraction, which can partly supply this information, was undertaken. It showed that the average value obtained indicated the predominance of a 2-layer hydrate. For water contents lower than 30%, it was checked in previous investigations that this was the usual hydration state of the interlayer in the MX-80 bentonite (Villar et al. 2012).

Acknowledgements

The research leading to these results received funding from the European Atomic Energy Community's Seventh Framework Programme (FP7/2007-2011) under Grant Agreement n°249681, the PEBS project. This work was additionally financed by ENRESA through a CIEMAT-ENRESA General Agreement. The laboratory work was performed by Ramón Campos and Juan Aroz, at CIEMAT. The X-ray diffraction tests were performed by Luis Gutiérrez-Nebot from CIEMAT and the mercury intrusion porosimetry and nitrogen adsorption tests in the CIEMAT laboratory run by Dr. Rocío Campos.

References

DELAGE, P. & LEFEBVRE, G. 1984. Study of the structure of a sensitive Champlain clay and its evolution. *Can. Geotech. J*. 21(1): 21-35.

ENRESA 2005. Ventilation experiment in Opalinus Clay for the management of radioactive waste. *Publicación Técnica ENRESA* 07/2005. Madrid, 82 pp.

Fernández, A.M. 2011. Determination of the Specific Heat Capacity of materials used as confinement barrier at El Cabril. Interim Report CIEMAT/DMA/2G208/3/11, 26 pp.

Gaus, I., Wieczorek, K., Mayor J.C., Trick T., García-Siñeriz, J.L., Schuster, K., Garitte, B., Kuhlman, U. 2011. EBS behaviour immediately after repository closure in a clay host rock: the HE-E experiment (Mont Terri URL). Proceedings of the 14th Int. Conference on Environmental Remediation and Radioactive Waste Management ICEM'11. September 25-29, 2011, Reims, France. P-59288. ASME, 7 pp.

GENS, A.; VALLEJÁN, B.; SÁNCHEZ, M.; IMBERT, C.; VILLAR, M.V. & VAN GEET, M. 2011. Hydromechanical behaviour of a heterogeneous compacted soil: experimental observations and modelling. *Géotechnique* 61(5): 367-386.

GUTIÉRREZ-NEBOT, L. 2013. Informe de caracterización de fases sólidas mediante XRD. CIEMAT, Residuos Radiactivos, Referencia 0430 0403 0306 0122 1119. Madrid, 26 pp.

IMBERT, CH. & VILLAR, M.V. 2006. Hydro-mechanical response of a bentonite pellets/powder mixture upon infiltration. *Applied Clay Science* 32: 197-209.

Johnson, L.H., Niemeyer, M., Klubertanz, G., Siegel, P., Gribi, P. (2002): Calculations of the temperature evolution of a repository for spent fuel, vitrified high-level waste and intermediate level waste in Opalinus Clay. *Nagra Technical Report* NTB 01-04. Nagra, Wettingen, Switzerland.

KARNLAND, O., MUURINEN, A., KARLSSON, F., 2005. Bentonite swelling pressure in NaCl solutions – experimentally determined data and model calculations. In: Alonso, E.E., Ledesma, A. (Eds.), Advances in Understanding Engineered Clay Barriers. *Balkema*, Leiden, pp. 241–256.

PEARSON F. 1998. Artificial waters for use in laboratory and field experiments with Opalinus Clay. *Paul Scherrer Institut TM* 44-98-08

Pearson, F. J., Scholtis, A., Gautschi, A., Baeyens, B., Bradbury, M., And Degueldre, C. 1999. Chemistry of porewater in matrix and faults. – In: Thury, M. & Bossart, P. (Eds.), Mont Terri Rock Laboratory: Results of the hydrogeological, geochemical, and geotechnical experiments performed in 1996 and 1997.

Plötze M., Weber H.P (2007): ESDRED: Emplacement tests with granular bentonite MX-80: Laboratory results from ETH Zürich. Nagra Arbeitsbericht NAB 07-24. Nagra, Wettingen.

SING, K.S.W., EVERETT, D.H., HAUL, R.A.W., MOSCOU, L., PIEROTTI, R.A., ROUQUÉROL, J., SIEMIENIEWSKA, T. 1985. Reporting physisorption data for gas/solid systems with special reference to the determination of surface area and porosity. *Pure & Appl. Chem*. 57(4): 603-619. IUPAC.

Teodori, S.P., Gaus, I. (Eds.) 2011. Long Term Performance of Engineered Barrier Systems (PEBS). Mont Terri HE-E experiment: as built report. Nagra Arbeitsbericht NAB 11-25. Nagra, Wettingen, 125 pp.

UNE 7045(1952): Determinación de la porosidad de un terreno.

VILLAR, M.V.; GÓMEZ-ESPINA, R. & GUTIÉRREZ-NEBOT, L. 2012. Basal spacings of compacted bentonite. *Applied Clay Science* 65-66: 95-105.

Villar, M.V.; Martín, P.L.; Gómez-Espina, R.; Romero, F.J. & Barcala, J.M. 2012. Long-term THM tests reports: THM cells for the HE-E test: setup and first results. PEBS Deliverable 2.2-7.1. CIEMAT Technical Report CIEMAT/DMA/2G210/03/2012. Madrid, 27 pp.